FRACTURE ANALYSIS OF MUS AND ADAIYAH FORMATIONS USING BOREHOLE IMAGE LOGS, ZAGROS BELT, NORTH OF IRAQ

A THESIS SUBMITTED TO THE GRADUATE SCHOOL OF APPLIED SCIENCES OF NEAR EAST UNIVERSITY

BY

BAYAR OTHMAN HASAN

In Partial Fulfillment of the Requirements for the Degree of Master of Science in Petroleum and Natural Gas Engineering

NICOSIA, 2020

BAYAR OTHMAN HASAN

FRACTURE ANALYSIS OF MUS ANDADAIYAHFORMATIONS USING BOREHOLE IMAGES

NEU 2020

FRACTURE ANALYSIS OF MUS AND ADAIYAH FORMATIONS USING BOREHOLE IMAGE LOGS, ZAGROS BELT, NORTH OF IRAQ

A THESIS SUBMITTED TO THE GRADUATE SCHOOL OF APPLIED SCIENCES OF NEAR EAST UNIVERSITY

BY

BAYAR OTHMAN HASAN

In Partial Fulfillment of Requirements for the Degree of Master of Science in Petroleum and Natural Gas Engineering

NICOSIA, 2020

Bayar Othman HASAN: FRACTURE ANALYSIS OF MUS AND ADAIYAH FORMATIONS USING BOREHOLE IMAGE LOGS, ZAGROS BELT, NORTH OF IRAQ

Approval of Director of Graduate School of Applied Sciences

Prof. Dr. Nadire ÇAVUŞ

We certify this thesis is satisfactory for the award of the degree of Master of Science in Petroleum & Natural Gas Engineering

Examining Committee in Charge:

Prof. Dr. Cavit ATALAR — Committee chairman, Petroleum and Natural Gas Engineering Department, NEU

Supervisor Prof. Dr. Salih SANER — Petroleum and Natural Gas Engineering Department, NEU

Assist. Prof. Dr. Süleyman AŞIR — Materials Sciences and Nanotechnology Engineering Department, NEU

I hereby declare that all information in this document has been obtained and presented in accordance with academic rules and ethical conduct. I also declare that, as required by these rules and conduct, I have fully cited and referenced all material and results that are not original to this work.

Name, Last name: Bayar Othman Hasan:

Signature:

Date: 29 July 2020

ACKNOWLEDGEMENTS

My great thanks go to my parents, my wife and my two wonderful sons for their personal supports and patience. Words cannot express how grateful I am for all sacrifices that you here've made on my behalf.

I would like to express my sincere gratitude to my principal supervisor Prof. Dr. Salih Saner for his valuable guidance and advices throughout the period of this research and for his suggestions that significantly improved this thesis.

I would like to take this opportunity to thank my committee member, Professor Dr. Cavit Atalar (Head of Petroleum and Natural Gas Engineering) for his support.

Last but not the least, I have special thanks to my manager James Hunt for his continuous support and help. Without his support it was almost impossible to finalizing this research.

To my love…

ABSTRACT

Fractures are planer discontinuities that result of brittle deformation in rocks. They are caused by tectonic and thermal stresses which are external and internal stresses respectively. The reservoir that contains natural fractures are known as fractured reservoirs. Fractures that are naturally occurred are present in most of the reservoirs and it is important to detect if the amount and the extent of these fractures are sufficient to affect the reservoir performance. The behaviors and characteristics that are the results of the existence of fractures could be detected and analyzed by borehole images.

Borehole image logs (BHI) can be used to detect and analyze structural features such as fractures, faults and bedding planes. Fracture attributes such as orientation, intensity, spacing and width (aperture) can be quantified planes. Extension, shear and tensile fractures are main fracture types. Generally, orientation, size and intensity of fractures are factors controlling the connectivity and affect the transmission of fluid in the reservoirs, Furthermore, mineralized reservoir fractures may act as a pathway for fluid or blockage the fluid flow. Borehole images identify the faults and fractures with different appearances and their extents along the depth of a wellbore.

This project investigates carbonate fractures in one of the oil fields in north of Iraq by image logs. The analysis of image logs is important for fracture modelling, reservoir characterization, drilling stratigraphy and optimizing production. The result of this research showed that the conductive open fracture systems, in all three wells, are striking NNE-SSW. Fracture intensity is much higher in the deviated well compared with vertical well and fracture system and they are better developed in the NW nose of the anticline compared to the SE region. Based on this study results, drilling deviated production wells (50º-60º hole inclination with WNW – ESE hole azimuth) is strongly recommended. This will help in optimising production rate by intersecting maximum fracture counts. It is recommended to drill with slightly lower mud weight for future drilling operation campaign to avoid borehole breakouts and induced tensile fracturing.

Keywords: Fracture; image log; conductive fracture; bedding; breakout; induced fracture.

ÖZET

Kırıklar kayalarda kırılgan deformasyon sonucu oluşan süreksizlik yüzeyleridir. Bunlar dıştan tektonik ve içten termal gerilimlerle oluşabilirler. Doğal kırıklar içeren rezervuarlar kırıklı rezervuarlar olarak bilinirler. Doğal kırıklar rezervuarların çoğunda mevcuttur ve bu kırıkların miktarının ve büyüklüğünün rezervuar performansını etkilemek için yeterli olup olmadığının saptanması önemlidir. Kırıkların davranış ve özelliklerinin tespit edilip analiz edilmeleri kuyu görüntüleri (borehole images) ile mümkün olabilmektedir.

Kuyu görüntü kütükleri (borehole image logs, BHI), kırıklar, faylar ve katman düzlemleri gibi yapısal özellikleri tespit etmek ve analiz etmek için kullanılabilirler. makaslama ve çekme kırıkları ana kırık tipleridir. Genel olarak, kırıkların oryantasyonu, büyüklüğü ve yoğunluğu aralarındaki bağlantıyı kontrol eden ve rezervuarlarda sıvı iletimini etkileyen faktörlerdir, Mineral dolgulu rezervuar kırıkları ise sıvı akışı için bir tıkaç olarak hareket ederler. Bu proje, Kuzey Irak'ta bir petrol sahasındaki karbonat kaya kırıklarının kuyu görüntü kütüklerinden incelenmesidir. Görüntü kütüklerinin analizi kırık modellemesi, rezervuar karakterizasyonu, sondaj stratigrafisi ve üretimin optimizasyonu yönlerinden önemlidir. Araştırma sonuçları, incelenen her üç kuyuda da elektriksel iletken olan açık kırık sisteminin NNE-SSW doğrultusunda olduğunu göstermiştir. Kırık yoğunluğu yönlü kuyuda, düşey kuyu ile karşılaştırıldığında çok daha yüksektir. Ayrıca antiklinal yapının KB ucunda GD bölgesine göre çok daha fazla gelişmişlerdir. Bu çalışma sonuçlarına göre, yönlü üretim kuyularının 50º- 60º eğimle BKB – DGD yönünde açılması önerilir. Bu sayede kuyuda maksimum sayıda kırık kesilerek üretim miktarı optimize edilebilecektir. Ayrıca kuyu ‘break out’larını önlemek için biraz daha ağır çamur kullanılması, buna karşın sondajla oluşan (indüslenmiş) tansiyonel kırıklarını önlemek için de daha düşük çamur ağırlığı kullanılması önerilir.

Anahtar Kelimeler: Kırık; görüntü kütüğü; iletken kırık; katmanlanma; breakouts; sondaj kırıkları.

TABLE OF CONTENTS

CHAPTER 5: CONCLUSIONS AND RECOMMENDATIONS

APPENDICES

LIST OF TABLES

LIST OF FIGURES

LIST OF SYMBOLS AND ABBERVATIONS

FMI: Formation Micro Imager

BHI: Borehole Image Log

XRMI: Extended Range Micro Imager

BHTV: Borehole Tele-viewer

FMS: Formation Micro Scanner

UHRI: Ultra-High-Resolution Resistivity Images

HMI: High-resolution Micro Imager

CBI: Circumferential Borehole Imaging Log

BBOE: Billion Barrel of Oil Equivalent

CMI: Compact Micro Imager

$\sigma 1$: Maximum Principal Stress

$\sigma 2$: Intermediate Principal Stress

$\sigma 3$: Minimum Principal Stress

σn: Normal Stress

σs: Shear Stress

3D: Three Dimensional

P10: Linear Density of Fractures (1D)

MD: Measured Depth

CHAPTER 1

INTRODUCTION

1.1 Background of Thesis

Fractures are structural features which is planar discontinuity formed from brittle deformation that exists in most of carbonate reservoirs and act as fluid conduit. The fractures that are naturally fractured can significantly impact the performance of reservoir. These fractures are either a pathway for fluid to flow, or they act as baffle or seal the movements (Fossen et al.,2007). Reservoir fractures are often neglected for consideration of calculations because of the complexity of technical work and the time effort. The denial of fracture would cause low technical and economic performance, so it is crucial to determine the existence of different types of fractures and their behaviour in reservoir in early stages of planning and evaluation (Nelson,2001). Recovery efficiency and productivity of the well is significantly affected by the natural fractures that exist in the reservoir (Narr et al., 2006).

The effects of fractures depend on their size which start from micro cracks to multi kilometre long fracture. They could be open and permeable which would act as conduit for fluid to flow (Narr et al., 2006). There are different types of fractures that act differently in the reservoir, and they have different behaviour toward the movement of the fluid, and those are shear, extension and tensile fractures (Nelson, 2001). The main factor effecting bulk permeability is the fracture connectivity. Understanding the connection of the fracture is important for measuring flow of fluid and storage potential (Pless, 2012). Length, density, orientation, spatial correlation and strain localization are the factors for the fracture network's connectivity (Nixon et al., 2012). Fracture patterns and their attributes, such as orientation, intensity, size and shape contribute to fluid flow in reservoirs bearing economic resources (oil, gas, water). Due to importance of the fracture in fluid transmission, it is necessary to study their patterns to quantify the fracture connectivity. Natural fractures are not randomly distributed and exhibit clustering patterns particularly in the damage zones around large-scale faults. Therefore, understanding the geometrical attributes of individual fractures is a crucial step in quantifying their connectivity. The attribute variations will be explored in terms of lithology and fault kinematics.

The selected field locations offer a natural laboratory to explore fracture patterns in the subsurface carbonate reservoirs (Priest et al., 1976). in this paper in order to detect and analyse the existence of fractures, their attribute and their distribution in the wellbore, the image logs have been studied. Then by displaying them on a flat surface by unrolling the digital image they are typically interpreted (Nar 2006).

Information on fractures such as dip, azimuth, aperture and morphology are obtained from borehole images. Resistivity borehole images such as Formation Micro Imager (FMI) logs can be used to interpret fractures and faults. The bright spots that appear on the image logs are conductive fractures, and they are interpreted as open and hybrid fractures and faults. The dark spots that appear on the image logs are resistive fractures, and they are interpreted as mineralized fractures and faults (Awdal,2015). The classification of fractures and faults are according to their appearance on the images as resistive.

1.2 Objectives of the Study

The aim of this thesis is to study the fracture distribution in the Mus and Adaiyah formations (Jurassic) in the Wells 2,3, and 4 in an oil field of NE Iraq. The analysis goes through integrating subsurface data, which are used to build up a conceptual fracture model.

Several wells have been drilled in the study field where almost all of them were productive and had good DST result but the last well DST was not very optimistic. The main goals for this research are:

- Quantify fracture attributes such as orientation, density, aperture from borehole image logs.
- Compare fracture attributes across wells in the selected field.
- Determine the measured depths of natural fractures and drilling-induced fractures.
- Using fracture analysis from BHI to determine optimum drilling trajectory where maximum fracture density can be encountered.

1.3 Problem Statement

Two criteria will be focused in the study:

1. Fracture attributes such as orientation can give indications about the paleo stress direction and the current in situ maximum horizontal stress (SHmax). Borehole breakouts are oriented perpendicular to the maximum horizontal stress direction while drilling induced tensile fractures are oriented parallel to the SHmax. Both breakout and drilling induced tensile fractures can be interpreted from borehole image logs. These interpretations can be used for geomechanical analysis. Furthermore, fracture orientation also helps to plan the well trajectory in naturally fractured reservoirs. It is generally assumed that best recovery is achieved from these fractured reservoirs where the well trajectory is perpendicular or at high angle to the open fractures. Fractures in such reservoirs can provide essential permeability or assist the permeability of the reservoir.

2. Seismic data do not detect any structural feature such as fractures below its resolution (20 m). Therefore, using borehole image logs can be used to analyze fractures and bedding. One of the benefits of fracture analysis from BHI is that fractures are clearly resolved and can be interpreted successfully.

1.4 Geological Setting

1.4.1 Tectonic setting

The present-day topographic relief of the Zagros fold and thrust belt is the result of a complex structural history that continues today. The geometry of the most significant and prospective structures is not simply the result of recent Cenozoic thrusting, but a product of the complex interplay between fault reactivation, basal and intermediate detachments and stratigraphic rheology. The position and orientation of fault trends influences the location, geometry and magnitude of structures observed in the field and subsurface. It is essential that all structures be interpreted within the context of plate rotations and the relative motions of the Eurasian and Arabian plates throughout the Phanerozoic period. The tectonic evolution of the Taurus-Zagros orogenic belt and the surrounding basins is fundamental to understanding the geometric, kinematic and temporal evolution of the hydrocarbon trapping structures as well as ascertaining the presence of source, reservoir and seal lithologies. The axis of the Zagros orogeny belt is oriented roughly NW-SE across the north-eastern margin of North Iraq and forms part of the Alpine-Himalayan orogenic system. The Zagros is divided into four zones based upon the degree and style of deformation. Foreland Zone, High Folded Zone, Zagros Imbricate Zone and Zagros Suture Zone (figure 1.2). The study area has been subject to contraction since the onset of continental collision during the Late Cretaceous. The principle contractional stress axis is orientated NE-SW and the resulting permanent strain has been accommodated by thrusting on, and folding above, various décollement surfaces at a number of stratigraphic levels. The degree of NE-SW shortening along the NW-SE axis of the Zagros orogenic belt does not appear to be consistent as the Mountain Front Flexure is not a linear feature; on a regional scale the front propagates further into the Foreland area (arcs) compared with other areas where the front has not extended as far. The main structural trends at subsurface in this study area, and in Phanerozoic units across the Arabian Plate, coincide with Precambrian N-S, NW-SE (Najd), NE-SW and E-W trending basement fault sets and structures (Jassim and Buday, 2006).

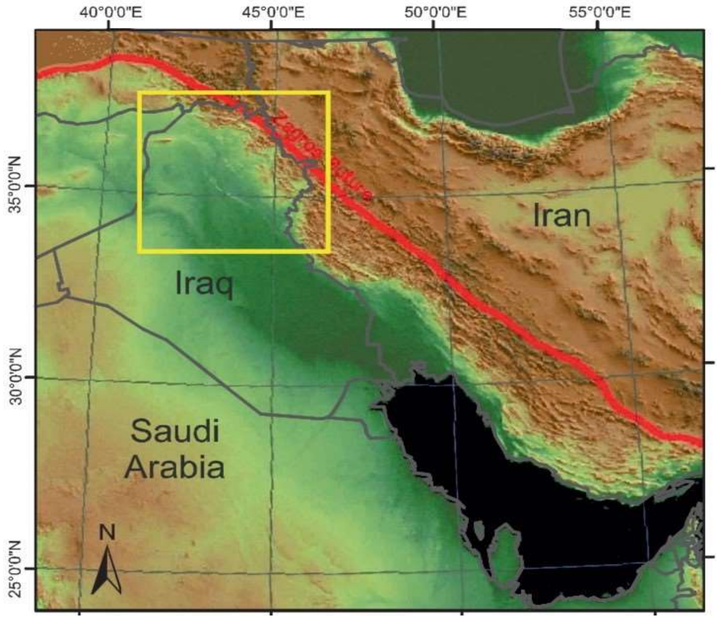

Figure 1.1: Regional tectonic map of the Zagros fold showing the location of study area (Awdal, 2016)

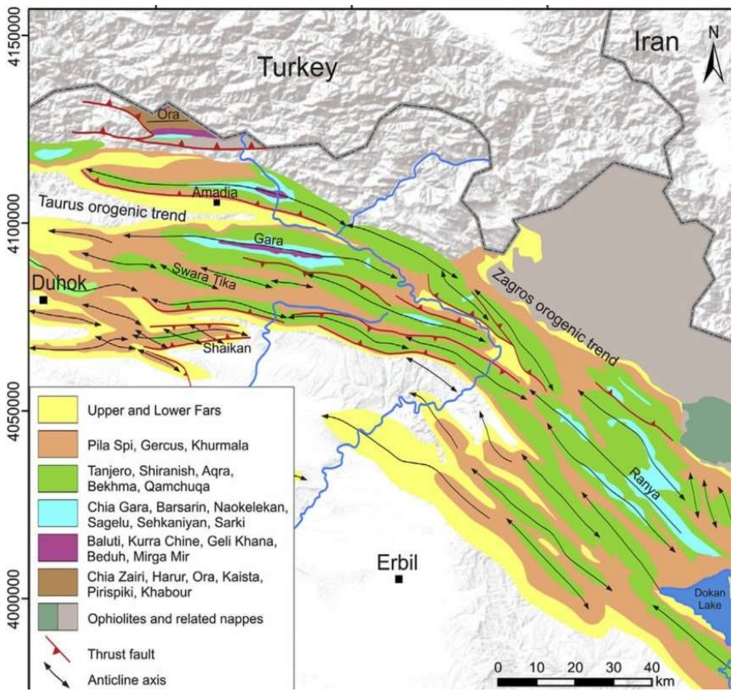

Figure 1.2: Simplified Geological map of North Iraq showing the anticline axes &related thrust faults in the study area (Awdalet al., 2016)

1.4.2 Stratigraphy

The stratigraphy of the North Iraq is shown in (Figure 1.3).The studied stratigraphic units are the Lower Jurassic Mus and Adaiyah formations. Both units are considered as fractured reservoirs in recent discoveries within North Iraq, and contain hydrocarbons within several fields such as Shaikhan, Atrush and Swara Tika. The surface equivalent to the Mus and Adaiyah Formations is the Sehkaniyan Formation (van Bellen et al.,1959). The Sehkaniyan Formation (Lower Jurassic) is exposed in the hinges of many anticlines in North Iraq. It is up to 350 m thick and consists of foetid, saccharoidal dolomites and dolomitised limestones. The Mus formation is recognized by a change in lithology, away from the mainly anhydritic lithology of the overlying Alan Formation to a predominantly limestone lithology of the Mus Formation. The top of the Mus is set at the base of the lowest significant bedded anhydrite of the Alan Formation overlying the limestone of the Mus Formation. The contact is conformable but can be gradational. The Mus formation is well known regionally and consists of intercalated marly limestones, occasionally pseudo oolitic pellety, with intercalations of calcareous shales towards the base and variable degrees of dolomitization and recrystallization. In some areas the limestones can be highly carbonaceous / organic with various degrees of oil staining. In some areas the limestones show evidence of mineralization, possibly indicating fractures. The lower part of the formation can be developed as green, pyritic calcareous shales in some well-sections. The Mus formation is considered to have been deposited in a transgressive marine environment with a very wide area of distribution. Fossils are abundant and based on the presence of the foraminifera Nubculania ssp, Nodopthalimidium spp and agglutinates the age is determined as Toarcian. The Mus formation has a gradational and conformable contact with the underlying Adaiyah Formation and is set at the top of the highest bedded anhydrite, which is reflected in the change from inorganic anhydrite sedimentation to deposition of the richly fossiliferous Mus limestone. The Adaiyah Formation can be identified by a change in lithology from the predominantly limestone Mus Formation to the anhydrite dominated Adaiyah Formation, although limestones are still present the Adaiyah Formation. The contact is conformable and often gradational, with the top considered to be the first significant anhydrite bed below the Mus Limestone. The Adaiyah Formation is an anhydrite dominated sedimentary unit with interbedded carbonates, shales and marls. The carbonates are usually limestones but can be highly dolomitized and recrystallized in certain areas. The middle part of the Adaiyah Formation can be more heterolithic with a significant increase in carbonates. Argillaceous material is common within this formation and can be present as individual shale beds or, which is more likely, finely dispersed within the main lithologies. The Adaiyah Formation is thought to have been deposited in an extensive evaporitic lagoonal environment. Fossils are infrequent, but rare Nodosaria sp., Glomospira spp. and lituolidsindet and the formations stratigraphic position suggest a Pliensbachian age. The basal contact with the underlying Butmah formation is conformable and gradational and is considered to be at the base of lowest considerable bedded anhydrite overlying the highest heterogeneous Butmah Carbonate.

The stratigraphic equivalent of equivalents of Mus and Adaiyah Formations in Saudi Arabia is Upper Marrot and Lower Marrot and in Kuwait its equivalent is Marrot.

In Wells the Mus & Adaiyah Formation are described as below
Formation: Mus (Lower Toarcian)
Depth: 3582m – 3644m
Thickness: 62m
The Mus Formation is a shallow-marine limestone deposited during a regional transgression. In Well 2 the Mus Formation is composed of a massive limestone, which is highly dolomitized within the top 10m with some dolomite beds. The limestone was quite variable texturally being described as mudstone to packstone, olive grey to brownish grey, occasionally dark brownish grey, sub blocky to flaky, cryptocrystalline, trace micritic patches, rarely slightly dolomitic, no visible porosity.

Formation: Adiayah (Pliensbachian)
Depth: 3644m – 3943m
Thickness: 299m

The Adaiyah Formation was likely deposited in a peritidal environment. It consists of interbedded dolomite and anhydrite, with some thin dolomitic limestone beds and rare claystone stringers.

From the drilled cutting samples the dolomite (60%) was described as mudstone to wackestone, varicoloured, moderate yellowish brown to greyish brown, medium dark grey to brownish grey, light grey to yellowish grey, hard to very hard, brittle, blocky to sub-blocky, predominantly crypto to micro crystalline, locally fine crystalline and micro sucrosic, variably calcareous and locally grading to calcareous dolomite, rare rhombic dolomite crystals, argillaceous in parts, locally anhydritic, locally micro fractures commonly filled with calcite and occasionally filled with disseminated pyrite, no visible porosity. The anhydrite (40%) beds were white to very pale blueish white, very light grey to very pale yellowish grey, opaque, rarely translucent, soft to firm, pasty, amorphous to sub-blocky, chalky text locally to common millimetric laminations and inclusions of dolomite and argillaceous material which are slightly calcareous.

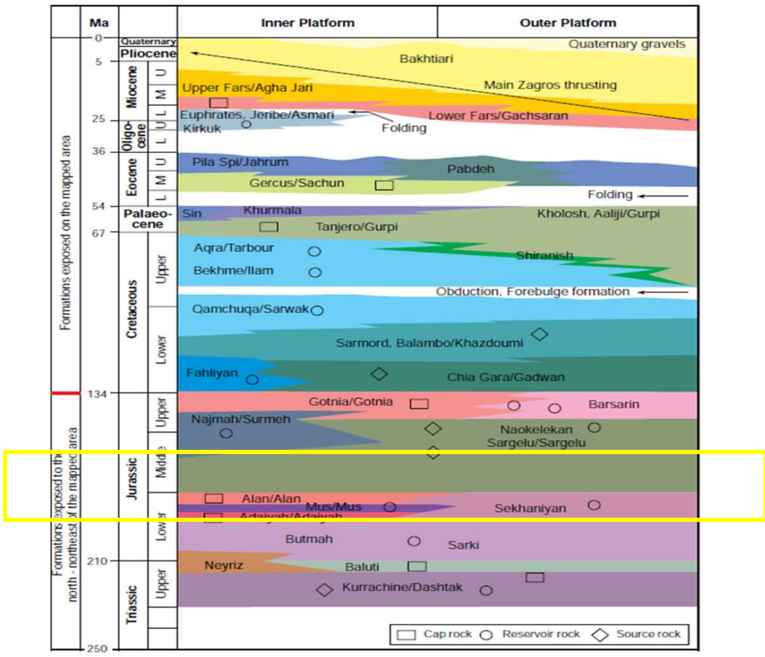

Figure 1.3: Stratigraphy of the North Iraq (van Bellent et al., 2005)

CHAPTER 2

LITERATURE REVIEW

Wong et al. (1989) Discusses that some tools such as Formation Micro Scanner (FMS), High-Resolution dipmeter and Borehole Televiewer (BHTV) have the capability of showing a clearer picture of the borehole. Most of the reservoir evaluation equipment are not able to detect thing beddings; therefore, it is not possible to evaluate production potential of small natural fracture accurately. Although it is hard with the help of the mention tools it is possible to have a good image of subsurface, but the interpretation of these borehole images relay on the quality of the image that presents data. In case bad quality image logs the thin bedding will not be identified. This paper proposed economical ways of enhancing the image log's quality.

Faraguna et al. (1989) documented that the borehole imaging devices could support the description of the reservoir by providing valuable information. Borehole image is used in fracture identification, thin-bed analysis and stratigraphic interpretation. In the paper ranges of devices used to obtain borehole images such as scanning devices and circumferential acoustic image devices were discussed. Circumferential devices scans the entire circumference of the borehole wall, and lithology changes such as fracture and vug, and borehole geometry variation alters the amplitude that provides the image. Although these devices provide images of borehole, there are limitations due to the quality of the images and the speed of logging. Circumferential Borehole Imaging Log (CBIL) is introduced to operate at higher data sampling rate which provides improved vertical and horizontal resolution.

Lambertini et al. (1992) Studied the quantification and identification of fracture using borehole images in Maracaibo Basin, Venezuela. The study shows that the Formation Micro Scanner tool (FMS) made an innovation in interpretation of characterization and description of the reservoir. The study added that with the latest development in fracture analysis, the center of the focus will be the modeling the fracture distribution in the reservoir.

FRACVIEW software has significantly promoted FMS images for quantitative analysis of fractures.

Sullivan et al. (1995) showed how to use a high-resolution and two-dimensional view of the borehole wall for examining fractured and thin bedded reservoir. He draws that the lack of calibration in the imaging tools causes mistakes in interpretations that were derived from image logs to qualitative. But in the latest studies of comparison between the interpretation of image log and core and production log, it supports that the application of image log data is quantitative. The paper concluded that according to the studies, the data which are provided by image logs could be interpreted for enhancing our capability for identifying the features such a fractured and thin bedded reservoir that directly effects the hydrocarbon reserves and the performance of the well.

According to Newberry et al. (1996) most of the methods for analyzing the dual porosity which contains fractures, vugs and molds depends on the resistivity and porosity logs, and this is unable to create such a result that corresponds with production due to the high complexity of the dual–porosity nature. This paper examines that borehole electrical images to provide small-scale resolution and azimuthal borehole coverage to solve the heterogeneous nature of porosity component quantitatively. It was discussed that the porosity map of the borehole could be created from electrical images.

Williams et al. (2000) used borehole images in a horizontal well in UAE to analyze a fractured carbonate reservoir called Thamama group. Borehole resistivity images has been structurally analyzed to study the structural compartmentalization of a complicated reservoir that have faults. It’s been discussed that borehole image and open-hole responses of log has subcategorized this study area into four borehole image units. Bed boundaries and faults are the connection points between these units. The bed boundaries which are conductive and resistive stylolitic have been found in these units. Furthermore, electrical response and the appearance of the image are the classification of these features. Fractures that show low resistivity are considered as cemented might block the fluid flow. Fractures that show resistivity are considered as their aperture is filled by a drilling fluid that is electrically conductive, might act as a path for fluid to flow.

Özkaya (2003) presented a method for estimation of the length of fractures by borehole image logs. He shows that essential fracture characteristics for hydrocarbons such as fracture connectivity and permeability need the knowledge of the mean length of fracture, and length distribution.

Gasc-Barbier (2010) states that the borehole images is a very beneficial method for gaining the discontinuity properties, but he also states that the limitation of the application should not be neglected as it has a huge impact on the results. He shows the inaccuracy of the borehole image by making a comparison between core sample and borehole images in the fracture network knowledge. The evidence of biases that has been encountered by borehole images are not negligible. For example, the core sample that shows 32% of fractures measure on borehole samples did not have any traces on the borehole images.

2.1 Background

Fractures are planar mechanical discontinuities in rocks and minerals that's caused by brittle deformations that's been cause by external and internal stresses. Creation of a fracture requires a stress to exceed the strength of the rock. Fracture is one of the important features in the reservoir that sometimes may get neglected despite the fact that it has been estimated 21 Billion Barrel of Oil Equivalent (BBOE) is present in different types of fractures. This denial is due to the complexity of technical work and the time effort and value of exploration and production. The denial of fracture causes a low technical and economic performance, so it is important to determine the effect of the fracture in the reservoir in early stages of planning and evaluation are done in an accurate way (Nelson, 2001). Natural fractures have different effects on the performance of primary, secondary and enhanced oil recovery. Fractured reservoir is a reservoir which has a natural fracture that has a significant effect on the fluid transmission as well as effects on the permeability or reserve or increased anisotropy of permeability. Three basic types of evaluation that require qualitative and quantitative data must be considered in any fractured reservoir analysis (Nelson, 1982) that are(1) Exploration evaluation to determine net reservoir quality; (2) Economic potential evaluation such as reserve and flow rates; and (3) Recovery evaluation for reservoir modeling.

2.2 Fractures

Rocks contain brittle and elastic deformations, and they undergo shattering, cracking, splitting and more importantly, fracturing if they are subjected to deviatoric stresses. They bear elastic deformation until failure. Fracture seen in figure 2.1 also present in all out crops. They are also present in most of the reservoir, so all reservoirs are considered fractured until the opposite is proven. It is important to detect if they are in sufficient amount and extent to have an enormous impact on the reservoir's behavior. Fractures affect reservoir's economic viability and different branches of Petroleum Engineering such as data collection, drilling, well completion and enhanced oil recovery. It is crucial to consider fractures when estimating the reserves. The reservoirs which are naturally fractured are important because it affects the recovery efficiency and productivity of the well (Narr, 2006).

Brittle deformation is mainly found in the upper 10-15 kilometers of earth's crust (Fossen, 2010). Fractures vary in size starting from micro cracks to multi kilometers long. They could be open and permeable or their aperture is filled by fine grain material or has been filled by secondary mineralization (Narr, 2006). That has been suggested and modified by Geologic Analysis of Naturally Fractured Reservoirs, fractures are either detected in laboratory experiments or observed in outcrops(Nelson, 2001).

Experimental fracture classification is subcategorized into three types of fractures according to (Nelson, 2001)

1. Shear Fractures (slip surfaces, such as faults),
2. Extension Fractures (opening, such as joints fissure and veins),
3. Tensile Fractures,

Seemingly, during folding the subsequent fracturing is controlled by mechanical anisotropy of the strata that's been contributed by the existence of pre-fold fracture network in folded rocks. Fracture orientations that are related to folding are controlled by the orientations of pre-folding fractures (Bergbauer and Pollard, 2004).

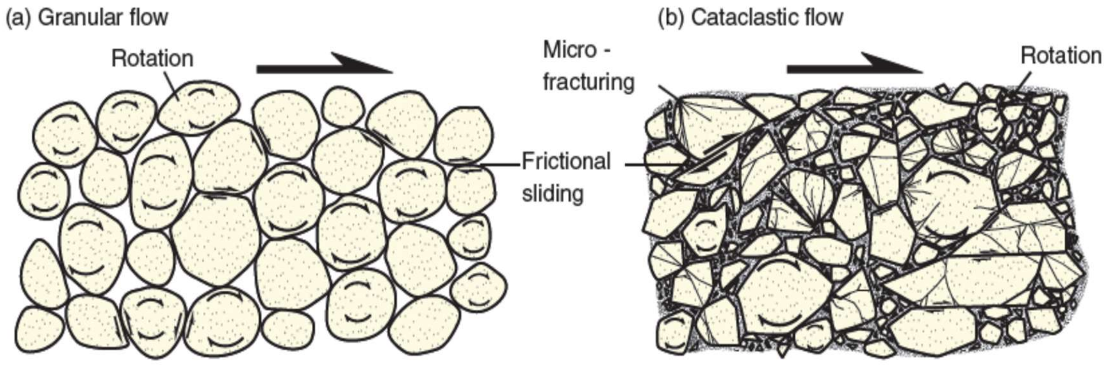

Figure 2.1: Brittle deformation mechanism (Fossen, 2010)

2.2.1 Shear fracture

A shear fracture is a relative displacement parallel to the plane of the fracture Figure 2.2; Figure 2.3. It typically develops at 20-30º to maximum principal stress (σ1) (Fossen et al, 2007; Fossen, 2010). If the displacement is in millimeter to decimeter it's still fault called shear fracture and it is called fault if the displacement is in larger scales, and slip fracture is used for fracture with parallel movement without considering the amount of displacement, whereas fault is a fracture with opposite sides is displaced parallel to the plane's surface (Narr, 2006). Generally, rocks are ought to undergo shear fracture rather than any other type of fractures. Furthermore, faults could prevent the flow of fluids in the reservoir, but it's also possible that it would help it to increase the flow through the rock locally figure 2.4. It depends on the texture of material, composition and aperture of the faults.

Based on (Narr, 2006) Faults are divided into three main types Figure 4.

1. Normal Faults,
2. Reverse or Thrust Fault,
3. Strike Slip Faults

Under temperature and pressure corresponding to upper part of lithosphere shear fracture is forming. Brittle-plastic transition is also a place for shear fractures to be formed where they are ought to grow into wider zones of cataclastic flow (Fossen, 2010).

2.2.2 Extension fractures

Extension fractures are the predominant fracture type in the fault damage zones figure 2.2. Several high intensity fractures are combined at damage zone where they are linked.

Extension Fractures occur under conditions of no to low confining pressure and low differential stress. They form perpendicular to minimum principal stress ($\sigma 3$) in terms of stress and perpendicular to the stretching direction under tensile conditions in terms of strain. In addition, extension fractures form parallel to the maximum principal stress axis during compressional setting. When extension fractures occur under conditions where at least one of the stress axes are tensile, then such fractures referred to as tension fractures. Under tensional stress of negative magnitude of $\sigma 3$ where tensile fractures form, extension fractures form under compressional stress of positive magnitude of $\sigma 3$. Similarly, tensile fractures can form at depth, where the effective stress is reduced by high fluid pressure (Gluyas and Swarbrick, 2004). Extension fractures form under compressional stress (positive magnitude of $\sigma 3$) whereas tensile fractures form under tensional stress (negative magnitude of $\sigma 3$). In addition, fluid expansion is potential for creating fractures at depth. Many other joints possibly form in relation to unloading and cooling of rocks. The cooling during uplift can potentially cause extension fractures in rocks. Joints are particularly common in competent layers in uplifted sedimentary sequences (Fossen, 2010). Joints can also form during burial and diagenesis in carbonate rocks.

2.2.3 Joints

Joints are the most common extensional fractures at the surface of the earth and involve very small strains. Joints mainly have microscopically detectable displacement across the joints surfaces thus they are considered as true extension fractures figure 2,2; figure 2,3. These extension fractures are filled with gases, fluids or minerals. Fissure is a term used for extension that is filled by air or fluid, while vein is used for mineral filled ones (Fossen, 2010). There is a distance between the parallel joints that has a huge impact on the effective permeability of the rock called joint spacing which acts as a pathway for the fluid.

In order to understand the mechanism of transportation of the reservoir fluid through joints the term Joint Set should be defined as a group of spaced joints that are parallel to each other.

Most of the joints are present in sets. When several joint sets are present in an area, it is called joint system. Thus, interconnected joints are a good pathway for the fluid to pass through. (Narr, 2006). It should be highlighted that joints and faults are two major natural types of fractures with different origin, characteristics, occurrences and effect on the reservoir fluid flow. The stress of the earth has controlled their orientation that have different direction and magnitude. In tight carbonate reservoirs, it is often concluded that the fracture system represents the entire pore volume for the reservoir and that these sets control the permeability or provide permeability for a low permeable reservoir.

2.2.3 Tension fracture

(Gluyas and Swarbrick, 2004). It typically develops perpendicular to minimum principal stress ($\sigma3$) in term of stress, and grow vertical to the extending path underneath tensile situations in terms of strain. Furthermore, extension fractures are parallel to the maximum principal stress axis in compressional setting. Extension fractures typically form below little or no limiting pressure. If extension fractures form below condition where at least one of the stress axes is tensile, then such fractures referred to as tensile fractures. Extension fractures form under compressional stress (positive magnitude of $\sigma3$) whereas tensile fractures form under tensional stress (negative magnitude of $\sigma3$). Tensile fractures can also

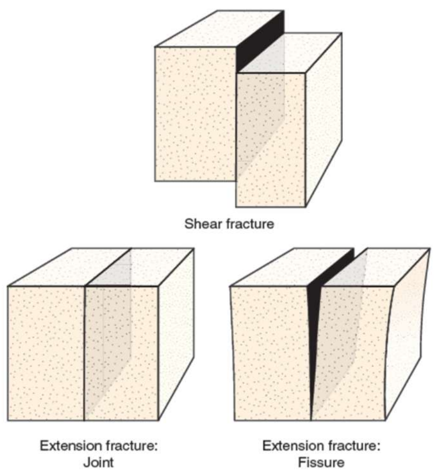

Figure 2.2: Three types of fractures: Shear, Extension fracture joint and Extension fracture fissure. (Fossen, 2010).

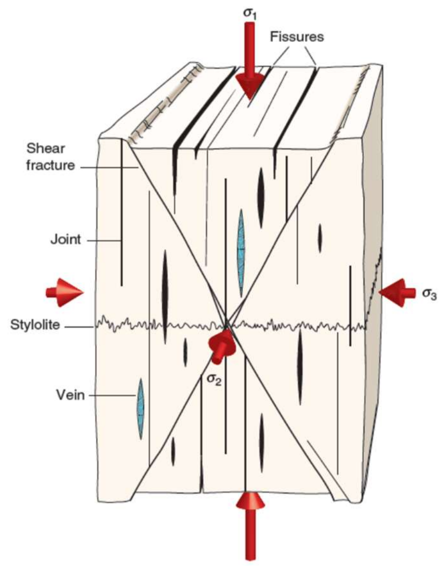

Figure 2.3: The orientation of various fracture types with respect to principal stress (σ_1) (Fossen, 2010)

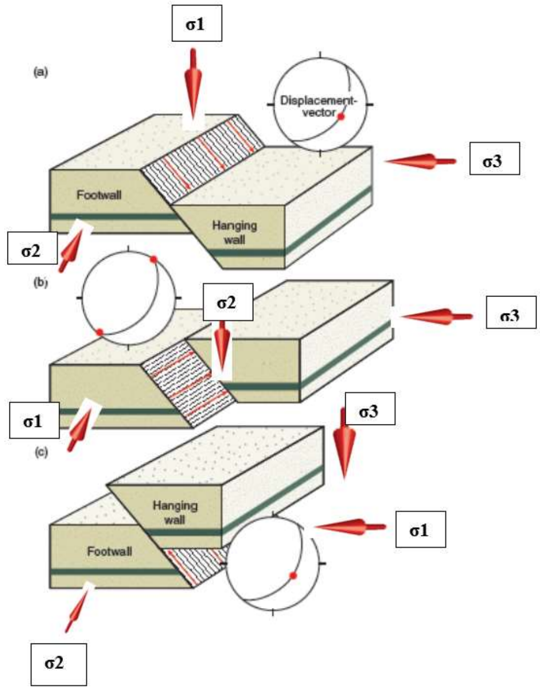

Figure 2.4: (a) is normal fault, (b) strike-slip fault, (c) reverse fault (Fossen, 2010)

2.3 Fracture Propagation Modes

Fracture mechanism is explained by four fracture modes. The first mode is the extension mode (opening) in which the displacement direction is perpendicular to strike of the fracture, the second mode is slip shear (sliding mode) that is parallel to the strike, and the third mode is open perpendicular to strike of the fault plane but up dip direction. In addition, contractional features uses mode four which is closing mode. Pressure solution and compaction such as stylolite and compaction bands are characteristic for this group. The combination of shear (second and third mode) and tension (the first mode) fracture is hybrid fracture (Figure 2.6). Hybrid shear fractures are mixed mode of transitional fractures that display both opening and shear modes (Ramsey and Chester, 2004; figure 2.5). For describing the condition of the stress of the rock that is necessary to induce the three basic types of fracture (extension, shear and hybrid) can use the Mohr's stress circle. For the formation of the hybrid shear fracture, the effective normal stress acting across the fracture planes are tensile, and they tend to be open (Price and Cosgrove, 1990). The horizontal and vertical axes on the Mohr diagram represent the shear (σs) and normal (σn) stresses that act on a plane through a point. The values of the maximum and minimum principal stresses ($\sigma 1$ and $\sigma 3$) are plotted on the horizontal axis, and the distance between $\sigma 1$ and $\sigma 3$ defines the diameter of the Mohr circle (Ramsey and Chester, 2004).

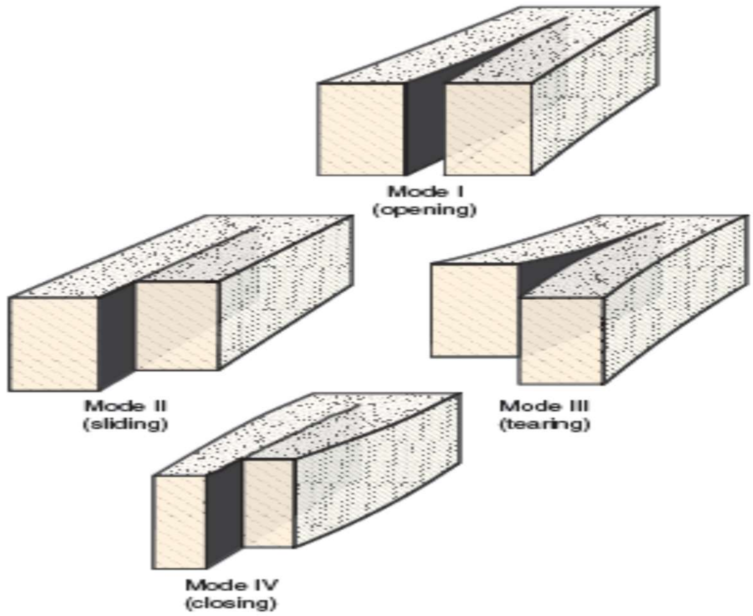

Figure 2.5: The four modes of fractures (Fossen, 2010)

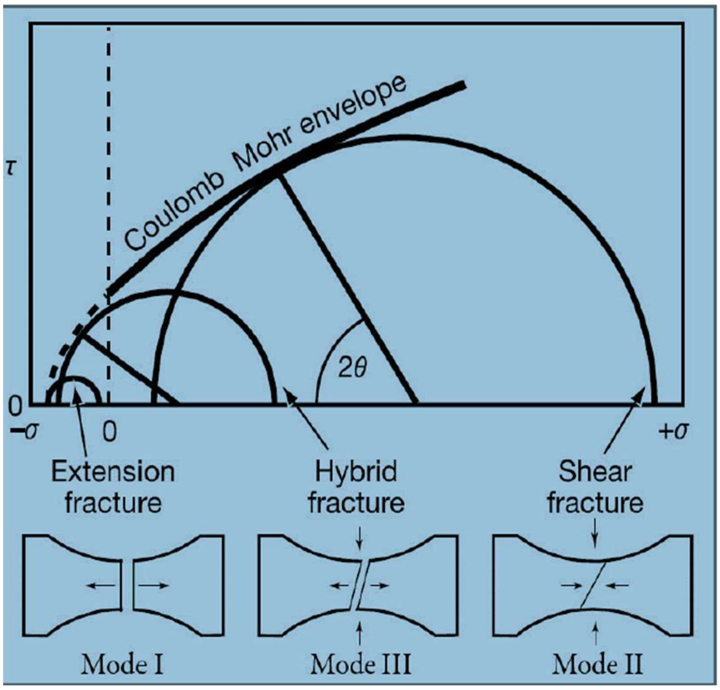

Figure 2.6: Mohr Columb circles for extensional, hybrid, and shear fractures. In the Mohr diagram, the fracture surface orientation is identified by the slope of the failure envelope at the point of tangency (Ramsey and Chester, 2004)

2.4 Fracture Attributes and their Characteristics

Orientation, intensity, spacing, aperture, fill and connectivity are attributes that all the fractures contain. In order to understand the single fractures and full fracture networks, the analysis of attributes is required. The fracture attributes provide understandings on the geometry and spatial relationships through the studied fracture network.

2.4.1 Spacing (Density)

Fracture spacing, as sampled along a 1-D scan line, is the distance between two adjacent fracture traces (Gillespie et al., 1999). The average spacing of joints of a given scale tends to be remarkably consistent, and partly depends on the rock type and bed thickness in which the fractures are developed (Twiss and Moores, 2007). A frequency that is relatively proportional to bed thickness is showed by bed-confined joints. In thin beds joints are very closely spaced, whilst their spaces are wide in thick beds. The greater the length of the joint, the wider the stress shadow; therefore, the mention relation is reflection of joint-stress shadow width (Pluijm and Marshak, 2004). A fracture set can grow almost continuous spacing impeding growth of new fractures due to the overlap of the stress shadows between neighboring fractures. Though, in highly folded regions and in areas of tighter folds, the contrary can be found where their geometry is important. Additionally, joint spacing and lithology have a relation between them. All in all, in stiffer beds which tend to have smaller joint spacing the stress is larger for a particular strain. (Pluijm and Marshak, 2004).

2.4.2 Aperture (Width)

The width of the opening measured normal to the fracture surface is called fracture aperture, but it can also be filled by the secondary filling minerals. The main factor for categorizing the fracture aperture into open, partially open or closed is the nature of the fracture infill which affects the fluid flow through fractures (Neuzil and Tracy, 1981). For detection of the fracture porosity the fracture aperture is the key characteristic. In folded carbonates, fracture porosity ranges between 0.01% - 0.5% (Nelson, 2001). The weathering and solution processes result in false aperture width; therefore, measuring fracture aperture in outcrops are not correct, so the measurement of aperture at outcrops should be handled cautiously. Weathering does not affect the borehole core samples, so the measured values of aperture from these core samples are representing the accurate values of fracture aperture. The mineralized subsurface aperture will not be shattered at the surface and they hold their aperture, so the measurement of mineralized subsurface aperture is accurate. But the fractures that are not cemented will shatter at the surface and the measurements are not quite correct. Different minerals have filled the outcrop fracture during the years. In addition, the borehole images that measure the fracture aperture might not be the correct value because open fractures provide enough distinction to be resolved on the image logs and similarly, other fractures would be suppressed and poorly imaged. Therefore, open fractures resolved on the image logs have apparent apertures.

2.4.3 Orientation

The strike and dip angles of the fracture plane define the fracture orientation, and the strikes of several fractures that make a dominant fracture trend is called fracture set. Fracture sets and inferred orientation of the tectonic stress that produces fracture set is identified by the help of orientation of fractures. A single fracturing may involve more than one orientation of fractures. Fractures that are created in the result of folding and faulting event have symmetrical orientation to the fold or fault. The orientation of the tectonic stress that have formed these fractures can be indicated by fracture orientation, because the stress field and the rocks may have been rotated since that paleo-fracture forming event; Therefore, measuring fracture orientation has implications for indicating paleo-stress direction. The orientation of genetically related fractures may vary from one lithology to another. For describing the fracture surface as planes (3D) and rose diagram to describe the trend of the fracture strikes (2D) as shown in the Figure 2.7. Stereograms are used to present the orientation data on fractures graphically (Peacock and Mann, 2005).

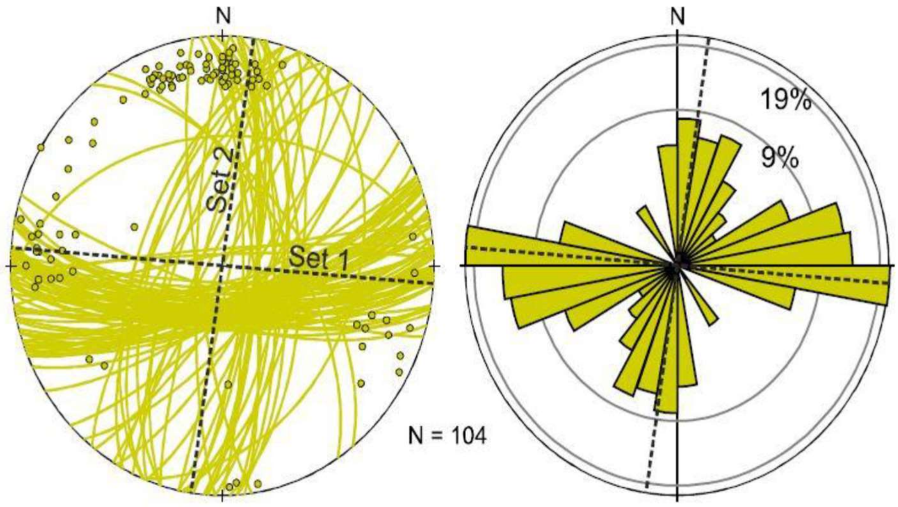

Figure 2.7: Stereogram and rose diagram of fracture strike orientations (Awdal, 2015)

2.4.4 Size (Height and Length)

The fracture terminates at tip lines of individual fracture, and they can be subcategorized into three types: tip abutted by overlying bed such as strata bound fractures; fracture abutting fracture; and tip in the intact rock. The ratio of the termination with fractures abutting another fracture in intact rock is very important for the reservoir connectivity and hence for the fluid flow. Fractures develop intersecting and branching patterns through time. There is different scale size where the fracture exists such as micro-fracture, macro-fractures, meso-fractures, and mega-fractures. Stratigraphy bound fractures usually follow log-normal size distribution in comparison to their length (Gillespie et al., 2001). The rock type and its structure are the main factor for defining the shape of the individual fractures in uniform rock the joint plane tends to have a circular or elliptical shape, with the long axis lying horizontal. In rocks with different mechanical properties such as interbedded sandstone and shale, joint height is confined by bedding and its length tends to be of much greater extent parallel to the bedding than across it. The fracture length is the length of a linear trace measured from the intersection of fracture to an outcrop surface (Twiss and Moores, 2007).

2.4.5 Intensity

The degree of strain and thickness and competency of the layers is fracture intensity. Fracture intensity is increasing towards the fault and it may also vary along the fault in a fault damage zone. Fracture intensity measurement varies per dimensions (Figure2.8) and the most popular conventions used for fracture intensity are defined according to (Dershowitz et al., 1992). One-dimensional fracture intensity (P10) is density of fractures. i.e. number of fractures per meter. It is often calculated from borehole image logs.

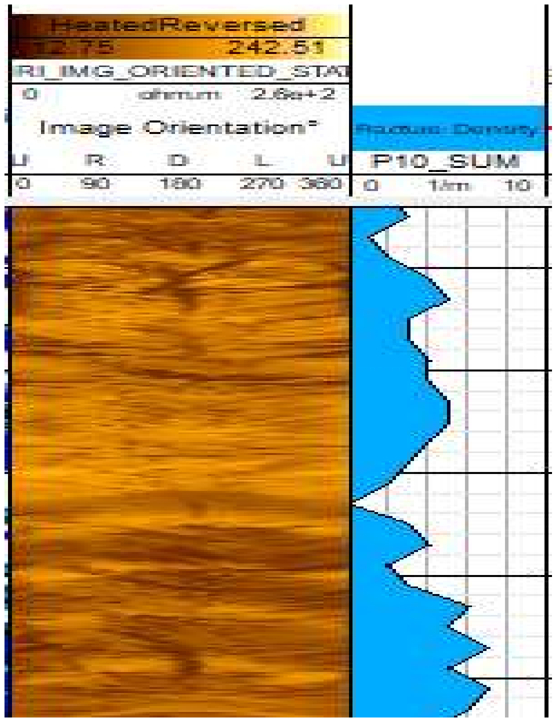

Figure 2.8: An example of a borehole image log showing 1D fracture intensity(P10)

2.4.6 Connectivity

Fractures can act as barriers or channels for fluid flow and consequently, understanding the connectivity of the fracture network is an important aspect for evaluating the fluid flow and storage potential within the studied fracture network (Pless, 2012). Fracture connectivity in this paper is primarily quantified using 2-D maps. The fracture network can be analyzed in terms of intersecting tips (X-nodes), abutting tips (Y-nodes) or isolated tips (I-nodes) used the relative proportions of I-, Y- and X-nodes to estimate connectivity within a fracture network. The connectivity of the fracture network is measured by the combined percentages of the X and the Y-nodes (Figure 2.9). The length, density, orientation, spatial correlation and strain localization determines the connectivity of the fracture networks, advocating that with increased deformation fracture connectivity also increases (Nixon et al., 2012).

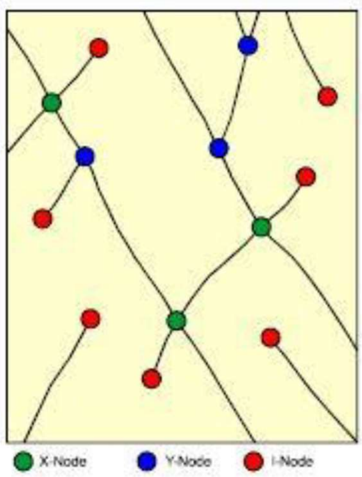

Figure 2.9: A schematic diagram showing an explanation of I, Y and X-nodes. The combined intersecting tips (X-nodes) and abutting tips (Y-nodes) make up the connecting nodes of any fracture network (Fossen, 2010)

2.4.7 Fracture fill

The space between two adjacent walls that is occupied by any material is called fracture infill. Common infill materials are minerals such as quartz, calcite and hematite, or fault rocks such as gouge, breccia or cataclast. The infill material can give an indication of the fluid types that have migrated through the fractures during their deformation history, and also offer valuable data about the relative timing of fracture-forming events. Separate deformation events with similar fracture orientations can also be differentiated by analyzing the cross cutting relationships between individual fracture infill sets.

2.5 Fracture Stratigraphy and Mechanical Stratigraphy

The term fracture stratigraphy is used where there is a positive relationship between fracture frequency and lithology (Hankset et al., 1994). Mechanical stratigraphy suggests that any stratigraphic unit with different rock types in layers will react mechanically different to stress, i.e. they have different strengths and Young's moduli. For example, a clay/shale layer can be exposed to a significant amount of ductile strain without fracturing, whereas a limestone or cemented sandstone will fracture at a considerably lower amount of strain. The consequence of this is that in a layered sequence fractures will initiate in certain lithologies while adjacent lithologies are unaffected. A stratigraphic unit that fractures independently from adjacent units is a mechanical layer, and fractures are typically limited to that particular mechanical layer abutting adjacent stratigraphic horizons, which are classed as mechanical layer boundaries (Wennberg et al., 2006).

2.6 Fracture Controlling Parameters

Controlling factures that effect the distribution, geometry and frequency of fractures within reservoir rocks include, but are not limited to, rock characteristics and diagenesis, structural geology and present-day factors (Peacock and Mann, 2005), (Figure 2.10).

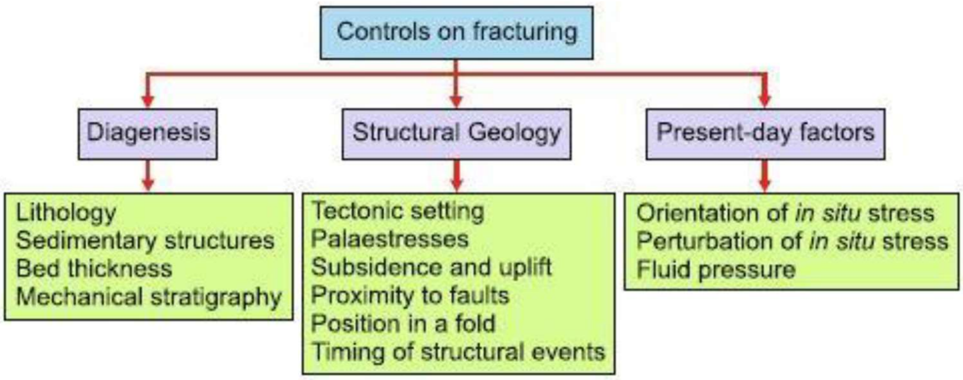

Figure 2.10: Summarized diagram of the main geological factors that control fracturing (Awda1, 2015)

Numerous geological factors comprising of grain size, mineral composition, porosity, bed thickness and structural position influence the density and spacing of fractures in subsurface rock units (Nelson, 2001). Grain size effects fracture density because generally finer grained rocks have lower permeability and higher strength than coarser grained rocks, resulting in a higher fracture density. Minerals such as quartz, feldspar and dolomite, which are some of the brittle components of rocks, can influence the spacing between fractures such that increasing strength and decreasing ductility could lead to more closely spaced fractures

(Peacock and Mann, 2005). Rocks of similar mineral composition and fabric can have varying porosity, which would influence the spacing and abundance of fractures within the rock, such that the lower porosity rocks will have closer spaced or more abundant fractures than the relatively higher porosity rocks. Fractures generally occur perpendicular to bedding planes in stratified rocks, so the bed thickness acts as a control on fracture density and orientation and there is a positive relationship between fracture spacing and bed thickness (Narr and Lerche, 1984).

CHAPTER 3
METHODOLOGY

3.1 Image Log Analysis

Image log analysis is used to detect the existence and distribution of fracture in the wellbore. The most important and useful source of data on location and orientation of fracture on the reservoir is provided by image logs. By displaying them on a flat surface and unrolling the digital image they are typically interpreted. Ellipse is formed by the intersection of the circular cylinder borehole with fracture when it's unrolled and flattened it will have a sinusoidal shape. Information on fractures such as dip, azimuth, aperture and morphology are provided by borehole images. Resistivity borehole images such as Formation Micro Imager (FMI) is obtained that come from subsurface oil fields. For fracture information the raw and processed data (i.e. DLIS files) from image log are used, and these data are interpreted by Techlog software. When the image log gamma ray is in match with wireline gamma ray, there will be no speed correction applying to the datasets. The images of pad were created and oriented relative to the north (Awdal, 2015).

The bright spots that appear on the image logs are conductive fractures, and they are interpreted as open and hybrid fractures and faults. The dark spots that appear on the image logs are resistive fractures, and they are interpreted as mineralized fractures and faults (Awdal, 2015). Induced fractures are often discontinuous, branched and quite irregular, and their direction tends to be in the orientation of principal horizontal stress. Tensile fractures in the orientation of maximum stress, and shear fractures in the direction of minimum stress causing breakouts are two types of induced fractures for inferring the current in situ stress direction which is an important stage to differentiate between natural and induced fractures uses breakout analysis. The structural dip was removed from image logs by filtering prevailing sedimentary influence in which bedding dips were used. Fracture spacing and fracture intensity (P10, P21, P32) as well as fracture porosity (P33) are calculated using Dip Counting Feature function in Techlog software (Schlumberger). Furthermore, fracture apertures were quantified which controls the fluid flow from the studied reservoirs where fractures are mostly productive

Several types of bed boundary, each with different image characteristics were identified. Conductive as non-stylolitic/weakly and stylolitic, Resistive bed boundaries are characterized by irregular to undulating traces with gradational margins and regular bed boundaries correspond to bed contacts between beds of different character, but where the contact itself is not decorated by marked image characteristics (Wanless, 1979).

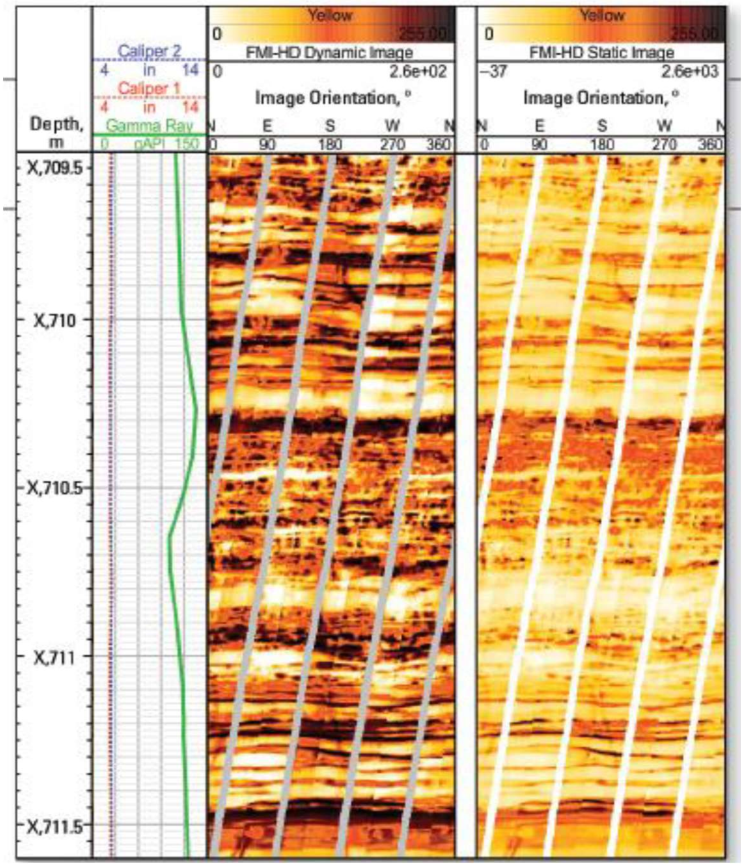

Figure 3.1: Image created by high definition formation micro imager (FMI – HD) Schlumberger tool (Yildirim and Goodlife, 2014)

3.2 Tools and Equipment

The following are a brief description of common image log tools:

3.2.1 Formation micro-imager - high-definition(FMI-HD)

High-definition Formation Micro-Imager (FMI-HD Schlumberger tool) has similar design as the industry standard Full-bore Formation Micro-Imager tool (FMI).

The FMI-HD is a four-pad micro-resistivity tool, with a flap articulated with each pad. Each of these pad and flap has 24 buttons (arranged in 2 rows of 12 buttons each). In total 192 buttons record high-resolution micro-resistivity data from which the image is generated at a sampling rate of 0.1 inch and an image resolution (button size) of 0.2 inch. When working in full bore mode, the tool provides continuous data with ~100% wellbore coverage in a 6.5-inch hole. In 8-inch hole the wellbore coverage is ~80%.

3.2.2 The formation micro-imager (FMI)

The Formation Micro-Imager (FMI Schlumberger tool) is a four-pad micro-resistivity tool, with 48 buttons per pad, for use with only water-based conductive mud and providing a sampling rate of 0.1 inch and an image resolution (button size) of 0.2 inch. When working in full bore mode, the tool provides continuous data with ~100% wellbore coverage in a 6.5inch hole, but only 53% wellbore coverage in a 12.25inch hole.

The FMI tool typically resolves cemented fractures (‘bright’-higher electrical resistivity than surrounding wall-rock) and fractures invaded by drilling mud (‘dark’-lower electrical resistivity than surrounding wall-rock). These fractures are referred to as electrically resistive (i.e. closed) and electrically conductive (i.e. potentially open) fractures, respectively. The FMI can detect open as large as the button size (0.2 inches) in the resulting images.

The Schlumberger Formation Micro Imager tool (FMI) consists of four caliper arms with a pad and flap at the end of each arm (Figure 3.2). The pads and flaps contain 192 resistivity sensors, 24 on each pad and flap, and the diameter of each resistivity sensor is 5 mm. Wellbore coverage of the FMI image is a function of hole diameter, the greater the hole diameter the less wellbore is imaged. The parts of the borehole that are not imaged appear as blank strips in the resultant logs

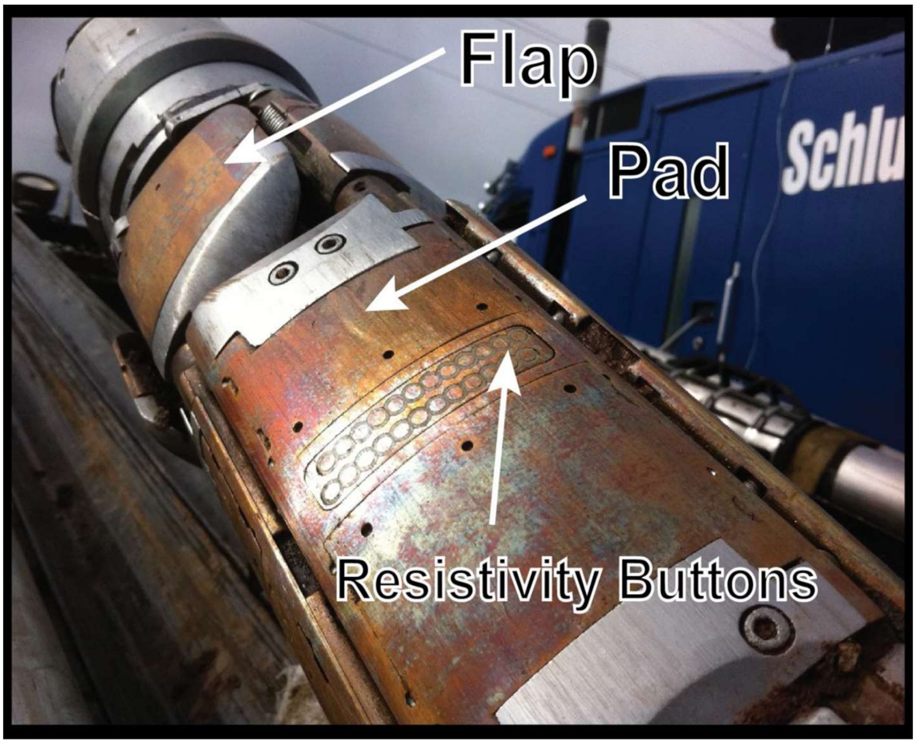

Figure 3.2: Formation Micro Imager (FMI) logging tool (Yildirim and Goodliffe, 2014)

The tools are run to the bottom of the well, then the pads are opened to press against the wellbore and logging commences from the bottom upwards. The resistivity of the formation is measured by passing an electrical current through the rock. The current passing through the rock is used to measure shallow and deep resolution resistivity components. Alongside the resistivity readings, the tool measures caliper, x-y-z axis accelerometer and compass readings, which are used for defining wellbore shape, borehole deviation and pad orientation.

3.2.3 X-tended range micro image (XRMI)

The X-tended Range Micro Image (XRMI Halliburton tool) is a water-based mud micro-resistivity tool which consists of pads mounted on 6 independently articulated arms with 25 buttons in each pad. The result is an image with 120 samples per foot and coverage of 67%

in 8 ½ inch holes. The XRMI tool provides a vertical sampling of 0.1 inch (2.5 mm) and a depth of investigation of 0.95 inch.

The XRMI tool typically resolves cemented fractures (‘bright’-higher electrical resistivity than surrounding wall-rock) and open fractures invaded by drilling mud (‘dark’-lower electrical resistivity than surrounding wall-rock). These fractures are referred to as electrically resistive (i.e. closed) and electrically conductive (i.e. open) fractures respectively. The XRMI can detect open fractures that have apertures ≥0.01mm.

3.2.4 High-resolution micro imager (HMI)

The High-resolution Micro Imager (HMI Weatherford tool) is a six-pad micro-resistivity image tool, with 25 buttons aligned in 2 rows per pad. In oil-based nonconductive muds, only 48 resistivity measurements are obtained, whilst in water-based conductive muds, 150 resistivity measurements are obtained providing a higher resolution image at a sampling rate of 0.1 inch (2.5mm) and an image resolution (button size) of 0.16 inch (4 mm). The borehole coverage varies with bit size; in a 6-inch, 8.5 inch, and 12.25 inch, the tool provides 79%, 62%, and 41% coverage, respectively. The HMI tool typically resolves cemented fractures (higher electrical resistivity than surrounding wall-rock) and fractures invaded by drilling mud (lower electrical resistivity than surrounding wall-rock). These fractures are referred to as electrically resistive (closed or mineralized) and electrically conductive (open) fractures, respectively

3.2.5 Compact micro imager (CMI)

The Compact Micro Imager (CMI Weatherford tool) is an eight-pad micro-resistivity image tool, with 176 buttons in total, of which 80 buttons in the upper four pads and 96 buttons in the bottom four pads are aligned in two rows in each pad. It provides a high-resolution image at a sampling rate of ~0.08 inch. The upper caliper arms are cross-linked helping to centralize the tool and provide two diameter measurements. The lower four caliper arms are independently articulated to maintain good borehole contact. They also provide four independent radii measurements.

3.3 Borehole Image Processing and Interpretation

The data is then processed to build up a resistivity image of the wellbore wall. Characterization of a particular fracture requires imaging by multiple sensors. The steps involved in processing the data are correcting the directional data for tool and hole azimuths, correcting for magnetic declination and applying accelerometer corrections to depth shift the resistivity traces such that different rows of resistivity sensors are in line where the same slice of the borehole was imaged. color maps are assigned to the borehole images based on ranges of resistivity values, with high resistivity fractures displayed as light colors and low resistivity fractures displayed as dark colors. Due to the difficulty involved in interpreting 3-Dimensional images, it is common practice to split the wellbore along true north and unroll the image until it becomes 2-Dimensional (Figure 3.3).

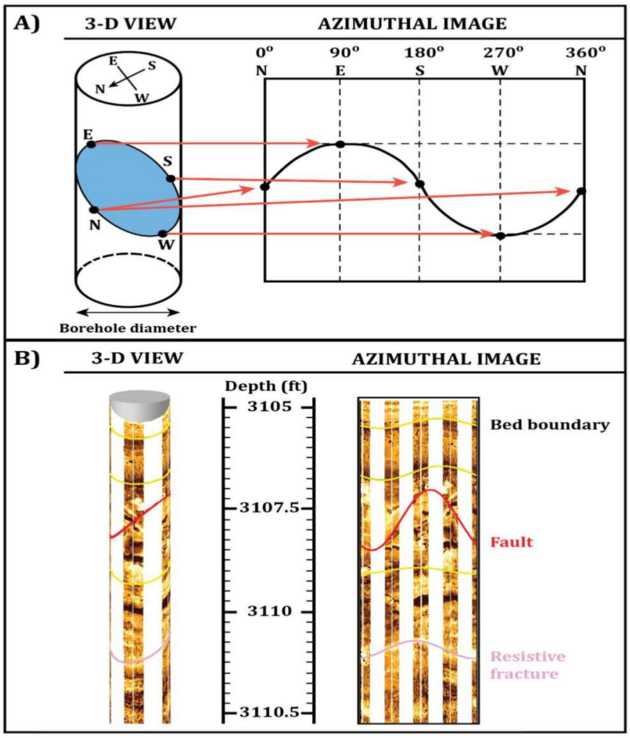

Figure 3.3: (A) Illustration of a cylindrical borehole intersected by a planar feature (B) A number of planar features were interpreted and color coded within a ~1.5 m (5.5 ft) section of FMI log. (Donselaar and Schmidt, 2005).

3.3.1 Data display

Once the data has been processed, a borehole image log is produced with both static and dynamic images. Static images have a single contrast setting that indicate relative changes in rock resistivity throughout the borehole, whereas dynamic images have variable contrasts providing enhanced images of geological features such as vugs, fractures and bed boundaries. waves are plotted for observed bed boundaries, fractures and other geological features. Azimuths and dips of planes geological features are presented in a tadpole plot (Figure 3.4).

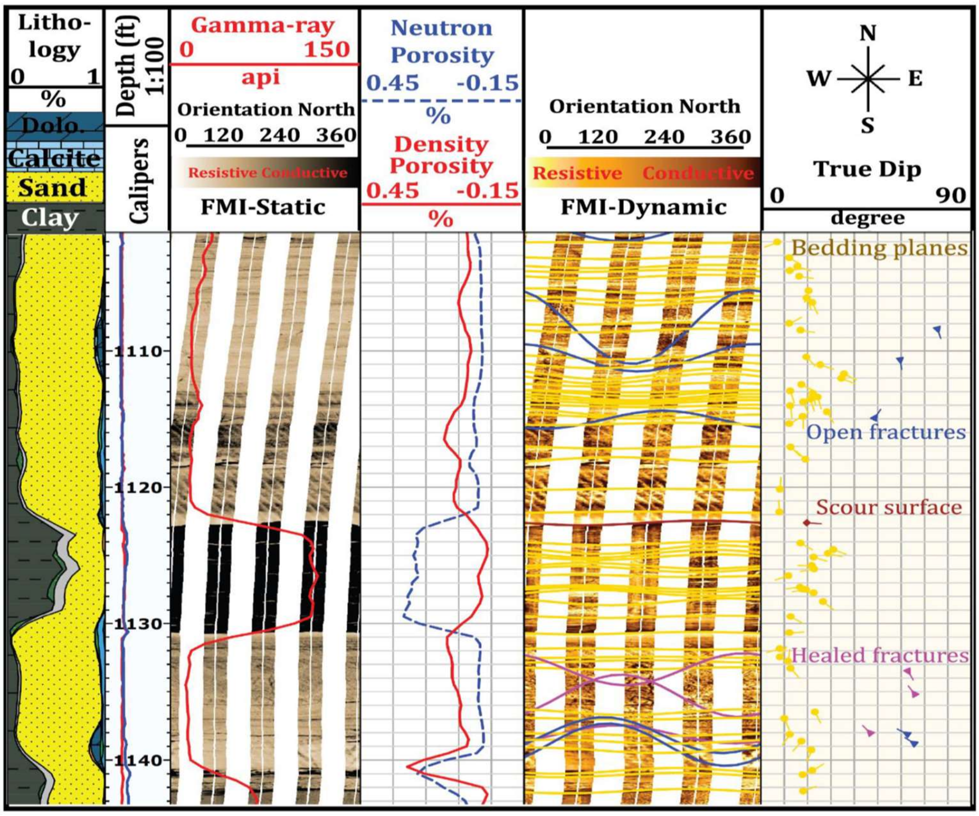

Figure 3.4: FMI resistivity image displays both open and healed fractures. Six tracks from left to right consists of lithology column. caliper measurements with a depth track, a static FMI image with a GR log curve, neutron-density porosity log curves& a dynamic FMI image a tadpole of geological feature (Yildirim and Goodliffe, 2014)

In regions of high stress, wellbore failures can be observed in the form of compressive and/or tensile failures. Also drilling induced tensile fractures can occur. Borehole breakouts are parallel to the minimum horizontal stress (Shmin) while drilling-induced fractures are parallel to the maximum horizontal stress (SHmax) for a vertical borehole (Figure 3.5).

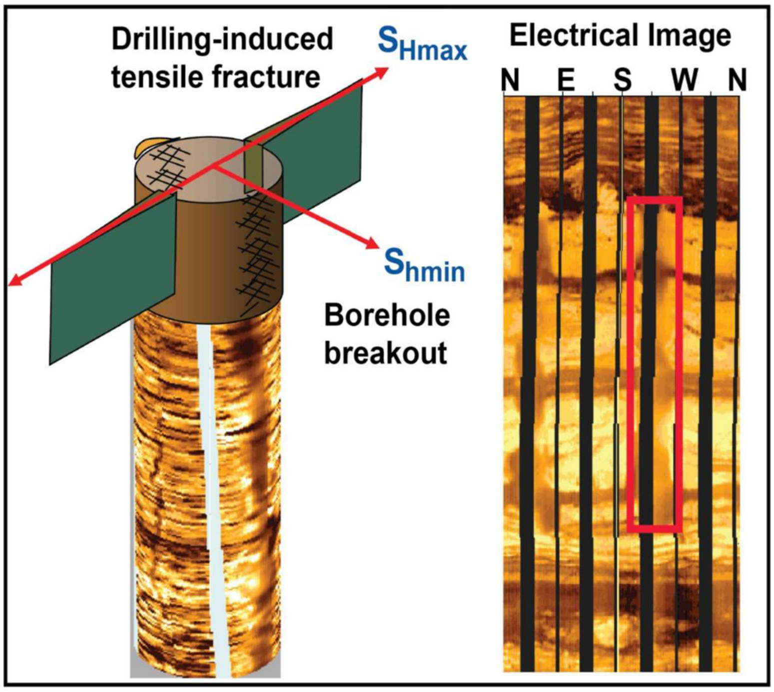

Figure 3.5: Borehole images showing borehole breakouts (red box on the right image) & drilling-induced tensile fractures on the wellbore wall (Soroush, 2010)

The four caliper arms on the FMI tool can also be used to interpret borehole breakouts. Used together with the FMI images these caliper profiles can be used to distinguish between stress-induced breakouts and other borehole enlargements, including washouts and key seats (Figure 3.6).

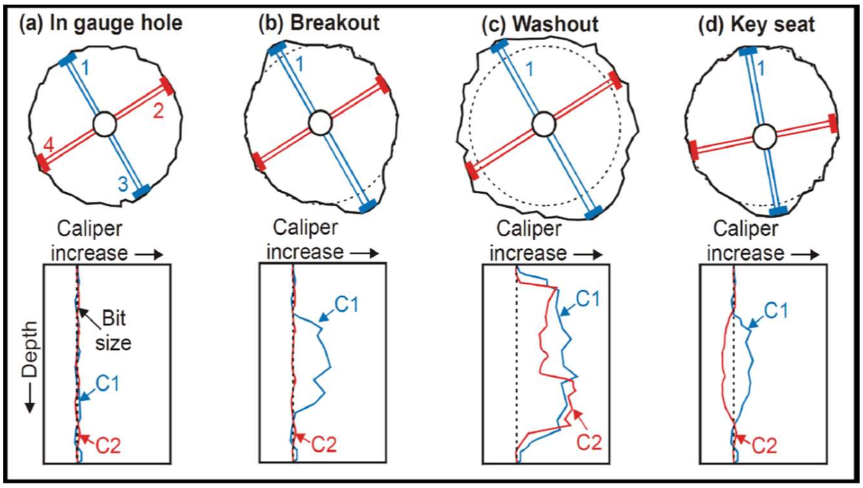

Figure 3.6: Categories of enlarged borehole and their caliper log responses (Reinecker et al., 2003)

3.3.2 Data interpretation methodology

The interpretation is completed using Schlumberger's Techlog software, an example of an interpreted section of FMI log is shown in Figure 3.4 The static FMI image in Track 3 clearly shows the differences in resistivity of the lithologies and is further highlighted by the Gamma Ray curve. The processed dynamic FMI image in Track 5 has sinusoid traces showing the dips of the interpreted geological features. The tadpole plot in Track 6 shows the direction and dip of beds in the formation together with tadpoles for any other geological feature that may be present (Table 1).

Table 3.1: Dip symbols used in FMI image interpretation

Dip Type	Symbol	Description
Bed boundary		Sedimentological, low angle planer features
Breakout		Conductive vertical enlargement on the wellbore wall
Conductive fracture		Structure generally high angle planer open features
Discontinuous Conductive fracture		Structure generally high angle planer half open features
Resistive fracture	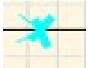	Structure generally high angle planer closed features
Drilling induced fracture		Conductive vertical planer features on the wellbore wall

CHAPTER 4
RESULTS AND DISCUSSION

4.1 Fracture Interpretation in Mus Formation in Well 2

Formation Micro Imager (FMI) raw data in Digital Log Interchange standard (DILS) format from Well 2 was imported into Schlumberger Techlog software and processed using the following steps: pad image creation, pad concatenation and orientation to generate the static image, and histogram equalization (normalization) to generate the dynamic image. Well2 is a vertical well and therefore the static and dynamic images were oriented with respect to geographic north. 37 fracture and bedding picks were interpreted from interval 2762-2797 m MD in Well. 2 Bedding planes are slightly tilted (2º-5º), reflecting the crestal structural position of the well and (Figure 4.1). Conductive (open) fractures are highly dipping (50º-80º) and their strike orientation is N-S. These open fractures are very important as they can provide essential permeability for fluid flow in Type II fractured reservoirs where matrix porosity is low. Furthermore, drilling induced tensile fractures have been also observed in the same interval. Such fractures are created when the drilling mud pressure exceeds the formation pressure or rock strength and consequently mud losses. Drilling induced tensile fractures are oriented NE-SW which are parallel to the maximum horizontal principle stress in the area (Figure 4.1).

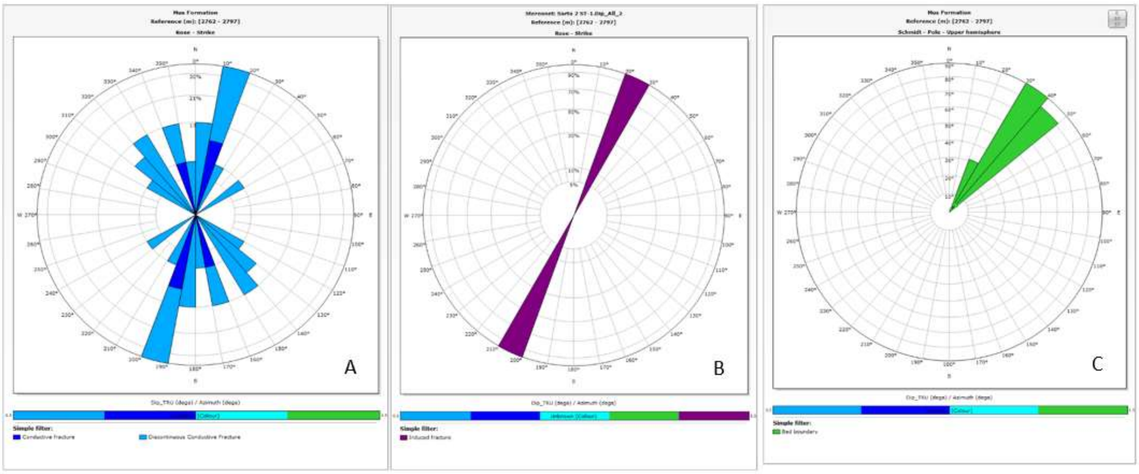

Figure 4.1: Rose diagrams of conductive fractures (A), induced fractures (B) and bedding planes dip direction (C), interpreted from FMI log in Well 2 within the Mus

The FMI image quality is good to very good at the interval of the Mus Formation. This is primarily due to the FMI coverage of ~80% in the 8.5” hole size diameter. Furthermore, fracture intensity which is defined as number of fracture counts per meter, is 3.3. In some other intervals, less fracture counts were observed. Fracture intensity is increased in the damage zones of the faults and in competent units such as limestone and dolomite. The Caliper log shows in gauge hole in the uppermost part and lower part of the Mus Formation. However, the interval between 2767-2779 m MD shows bad borehole condition due to breakouts and to less extent some washouts (Figure 4.2). The whole interval shows low Gamma Ray log reading (20-30 API) indicating clean limestone facies.

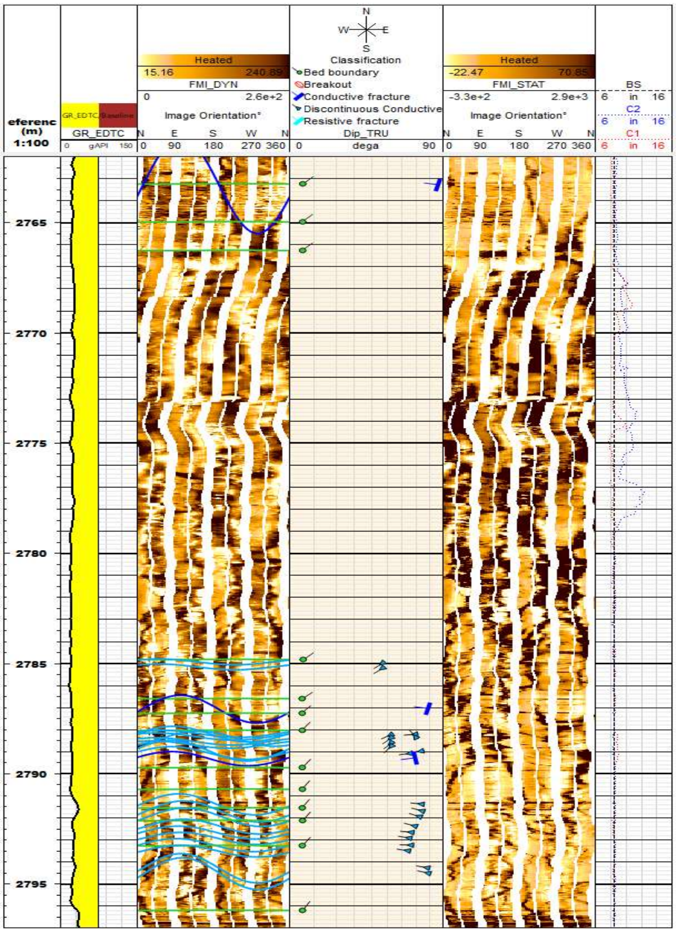

Figure 4.2: FMI static and dynamic logs showing conductive fractures, bedding picks &tadpoles interpreted from FMI log in Well 2 within the Mus Formation

4.2 Fracture Interpretation in Adaiyah Formation in Well 2

In the Adaiyah Formation which is underlying the Mus Formation, 137 fracture and bedding picks were interpreted from interval 2800-2930 m MD in Well2Bedding planes are slight tilted (<10º), reflecting the crestal structural position of the well and dipping towards NE (Figure 4.3). Conductive (open) fractures are highly dipping (42º-85º) and their strike orientation is NNE and SSW. These open fractures are very important as they can provide essential permeability for fluid flow in Type II fractured reservoirs where matrix porosity is low. Furthermore, drilling induced tensile fractures have been also interpreted from the same interval. Such fractures are created when the drilling mud pressure exceeds the formation pressure or rock strength and consequently mud losses occur. Drilling induced tensile fractures are oriented NE-SW which are parallel to the maximum horizontal principle stress in the area (Figure 4.3), whereas borehole breakouts are oriented NW-SE which are perpendicular to the NE-SW maximum horizontal stress. Borehole breakouts are shown on the FMI image logs in two stripes with 180ºangle of induced fracture are perpendicular to the breakout direction (Figures 4.3 and 4.4). The drilling induced tensile fractures and borehole breakouts are indicators to quantify the maximum horizontal stress and this orientation is often used in reservoir geomechanical studies.

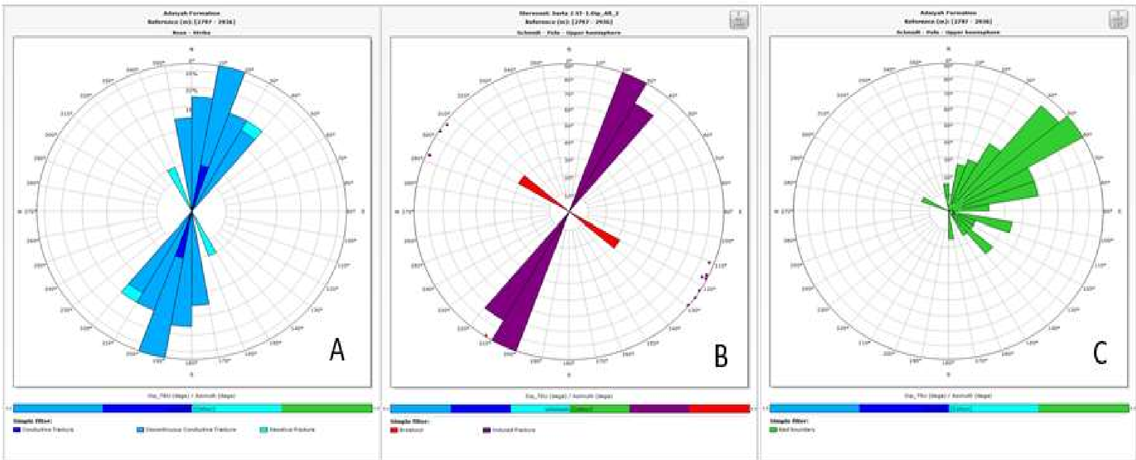

Figure 4.3: Rose diagrams of conductive fractures (A), induced fractures (B) and bedding planes dip directions (C), interpreted from FMI log in Well 2 within the Adaiyah Formation

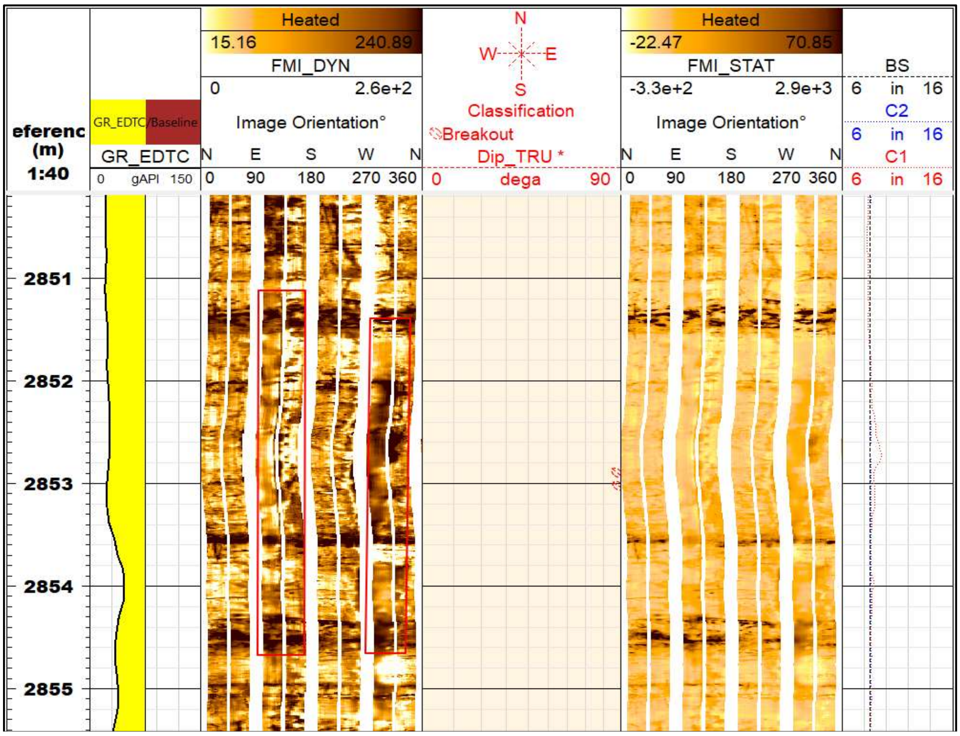

Figure 4.4: FMI static and dynamic logs showing borehole breakouts interpreted from FMI log in Well 2 within the Adaiyah Formation

The FMI image quality is good to very good at the interval of the Adaiyah Formation. This is primarily due to the FMI coverage of ~80% in the 8.5” hole size diameter. The caliper log shows in gauge hole at the most interpreted intervals e.g. 2882m – 2892 mMD (Figure 4.5). Furthermore, fracture intensity which is defined as number of fracture counts per meter, is 1.25 fractures/m. Fracture intensity is increased in the damage zones of the faults and in competent units such as limestone and dolomite.

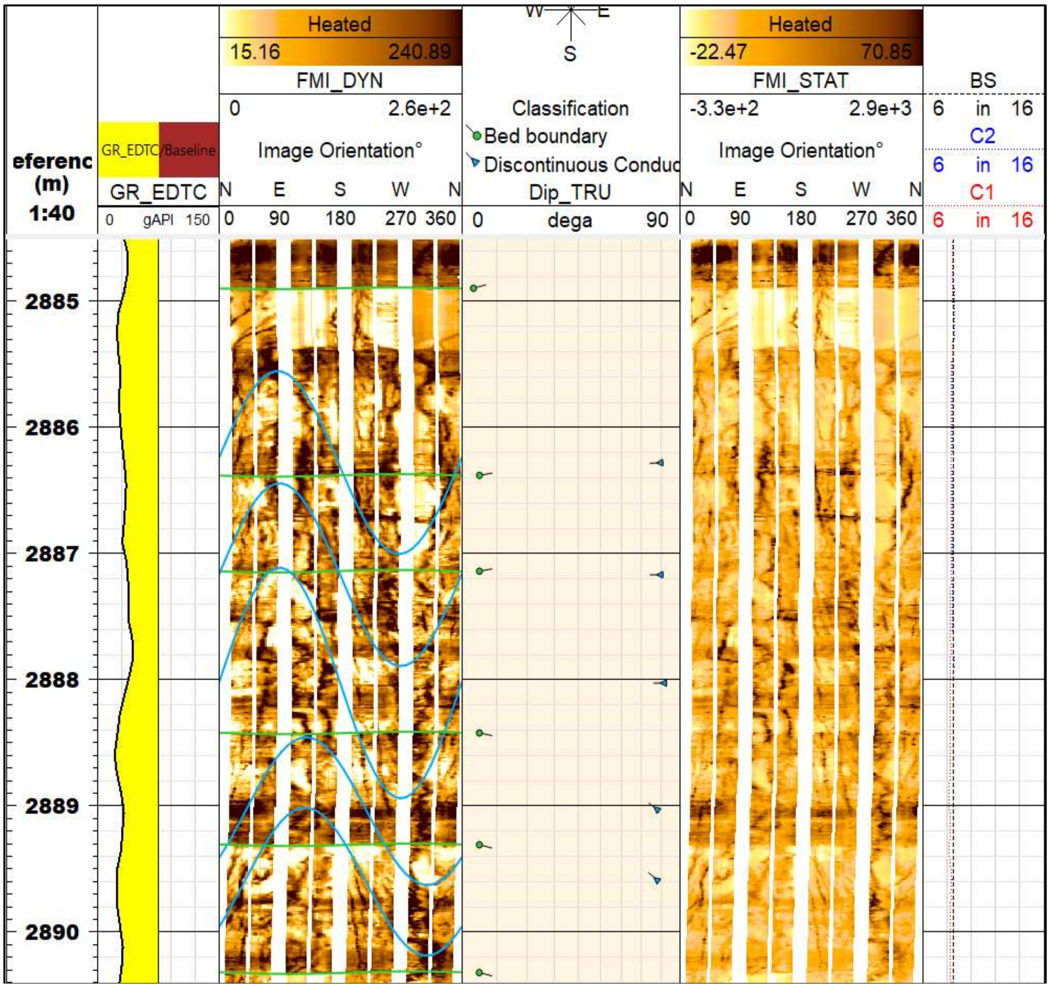

Figure 4.5: FMI static and dynamic logs showing conductive fractures, bedding picks & tadpoles interpreted from FMI log in Well 2 within the Adaiyah Formation

4.3 Fracture Interpretation in Mus Formation in Well 3

The raw data (DLIS file format) of ultra-high-resolution resistivity images of Well3 were imported into Schlumberger Techlog software and processed using the following steps: pad image creation, pad concatenation and orientation to generate the static image, and histogram equalization (normalization) to generate the dynamic image. Well3 is a deviated well (55º hole inclination at the TD) and therefore the static and dynamic images were oriented with respect to the high side of the well.

In the Mus Formation which is overlying the Adaiyah Formation, 288 fracture and bedding picks were interpreted from interval 3582-3644 m MD in Well2 bedding planes are low tilted (<14º), reflecting the crestal structural position of the well and dipping towards NNE (Figure 4.6). Conductive (open) fractures are highly dipping (65º-90º) comparing to Bedding and their strike orientation is NE-SW. These open fractures are very important as they can provide essential permeability for fluid flow in Type II fractured reservoirs where matrix porosity is low.

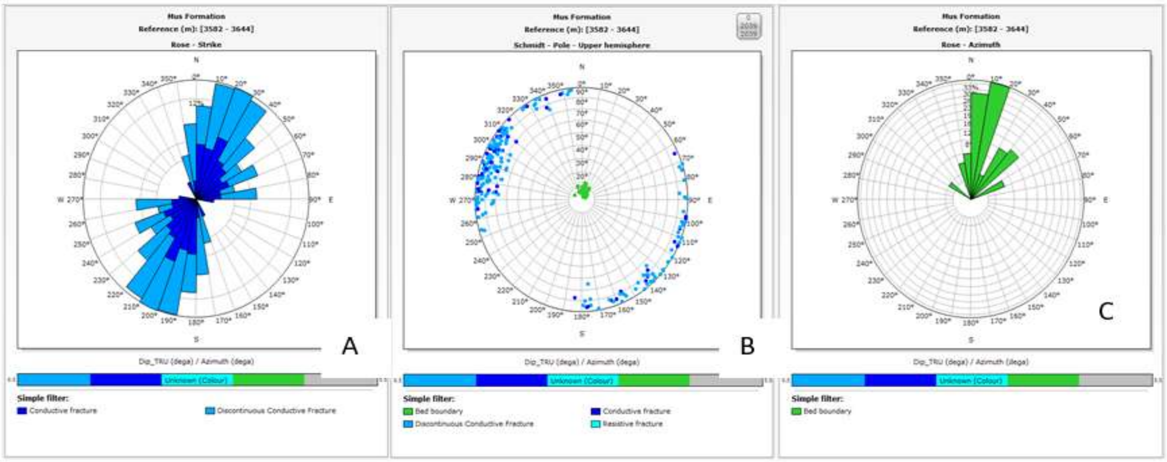

Figure 4.6: Rose diagrams of conductive fractures (A), pole to conductive & bedding (B) & bedding planes dip direction (C), interpreted from FMI log in Well 3 within the Mus Formation

The UHRI image quality is very good at the interval of the Mus Formation. This is primarily due to the full coverage of the UHRI image logs. Furthermore, fracture intensity is very high (up to 8 fractures/meter) in the interpreted interval 3582 – 3644 m MD (Figure 4.7). The high fracture intensity could be attributed to the well trajectory which is highly deviated (55º hole inclination) and a hole azimuth of 283º and since these fractures are sub-vertical, the well has intersected maximum number of fractures. The high fracture intensity has implications on well performance and production optimization.

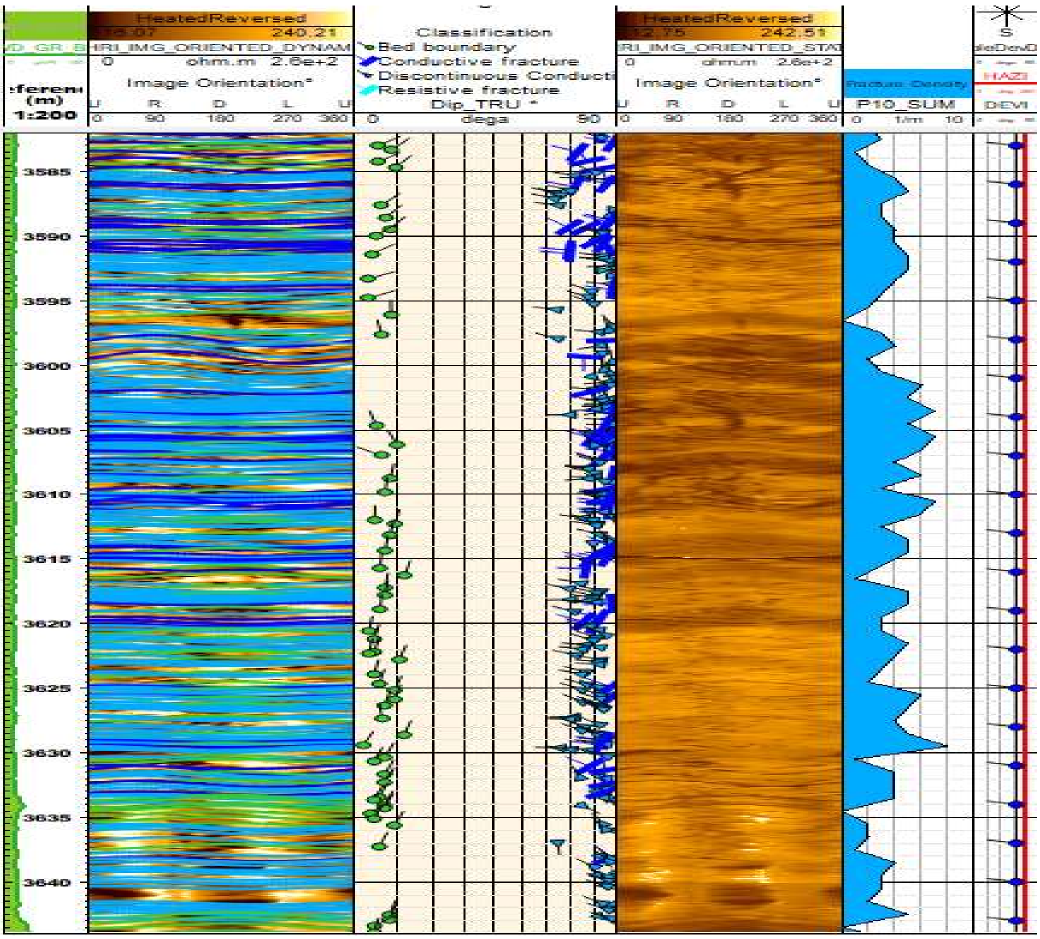

Figure 4.7: UHRI static and dynamic logs showing beddings and conductive fractures interpreted from the UHRI log in Well 3 within the Mus Formation. Fracture intensity is also shown in a separate log track entitled with P10

4.4 Fracture Interpretation in Adaiyah Formation in Well3

The raw data (DLIS file format) of ultra-high-resolution resistivity images (UHRI) of Well3 has been imported into Schlumberger Techlog software and processed using the following steps: pad image creation, pad concatenation and orientation to generate the static image, and histogram equalization (normalization) to generate the dynamic image.

In the Adaiyah Formation which is underlying the Adaiyah Formation, 1328 fracture and bedding picks were interpreted in the Adaiyah Formation in Well. 3 bedding planes are gently dipping (<16º), due to the crestal structural position of the well and dipping towards N (Figure 4.8). Conductive (open) fractures are highly dipping (70º-90º) comparing to bedding and their strike orientation is NE-SW. These open fractures are very important as they can provide essential permeability for fluid flow in Type II fractured reservoirs where matrix porosity is low.

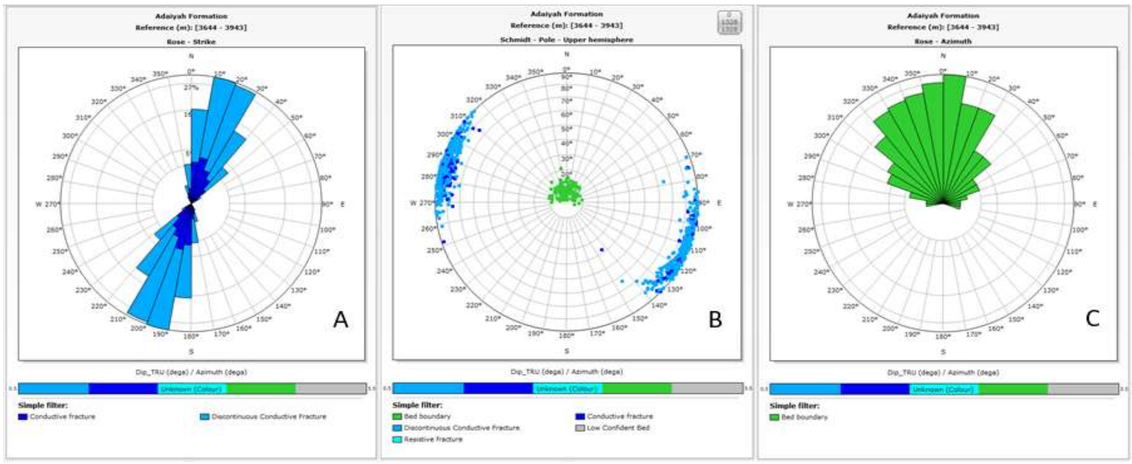

Figure 4.8: Rose diagrams of conductive fractures (A), pole to conductive & bedding (B) & bedding planes dip direction (C), interpreted from FMI log in Well 3 within the Adaiyah Formation

The UHRI image quality is very good at the interval of the Mus Formation. This is primarily due to the full coverage of the UHRI image logs. Furthermore, fracture intensity is very high (up to 10 fractures/meter) in the interpreted interval 3645 – 3940 m MD (Figure 4.9). The high fracture intensity could be attributed to the well trajectory which is highly deviated (55º hole inclination) and a hole azimuth of 283º and since these fractures are sub-vertical, the well has intersected maximum number of fractures. The high fracture intensity has implications on well performance and production optimization.

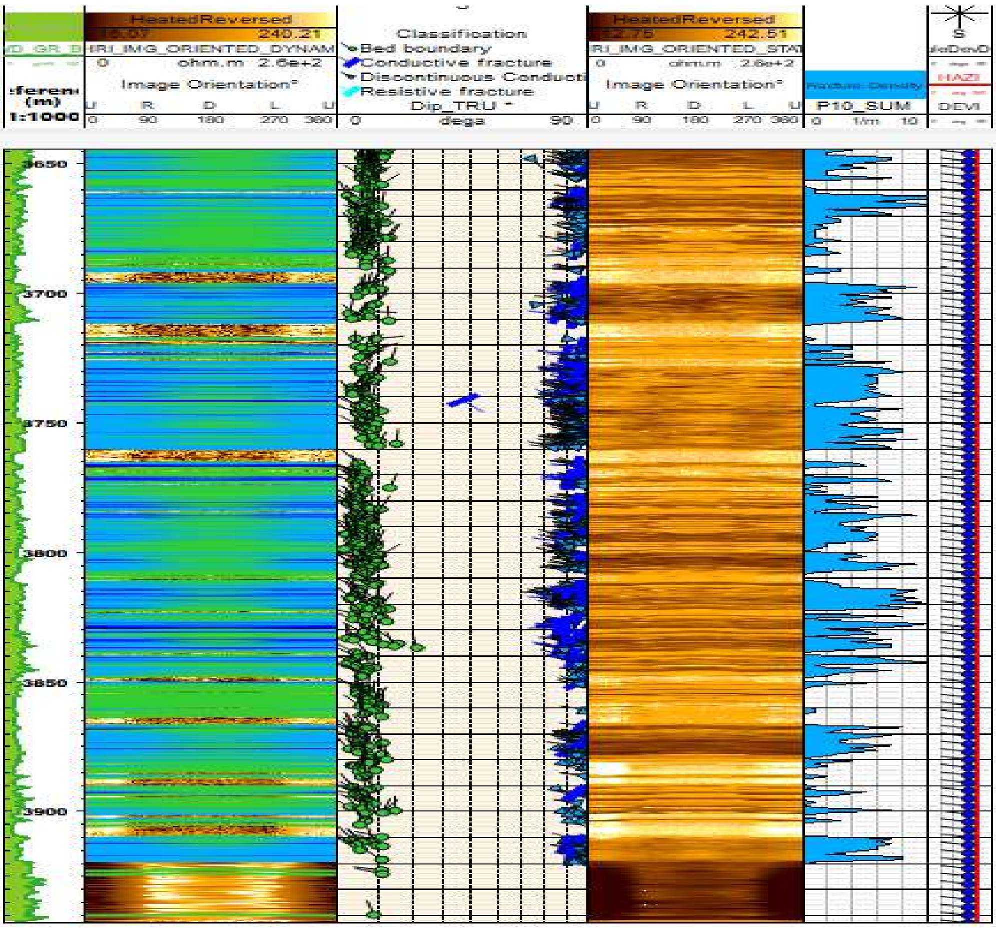

Figure 4.9: UHRI static and dynamic logs showing beddings and conductive fractures interpreted from the UHRI log in Well 3 within the Adaiyah Formation. Fracture intensity is also shown in a separate log track entitled P10

4.5 Fracture Interpretation in Mus Formation in Well 4

Formation Micro Imager (FMI) raw data in DLIS format of Well4were imported into Schlumberger Techlog software and processed using the following steps: pad image creation, pad concatenation and orientation to generate the static image, and histogram equalization (normalization) to generate the dynamic image. Well4 is a vertical well and therefore the static and dynamic images were oriented with respect to geographic north.

28 fracture and bedding picks were interpreted within the Mus Formation in Well3 Bedding planes are low angle (<10º), due to crestal structural position of the well and dipping towards N (Figure 4.10). Conductive (open) fractures are highly dipping (75º-85º) comparing to bedding and their strike orientation is NE-SW. These open fractures are very important as

they can provide essential permeability for fluid flow in Type II fractured reservoirs where matrix porosity is low. Furthermore, borehole breakouts have been also interpreted from the same interval. Borehole breakouts are wellbore instability fractures and they are oriented NW-SE which are perpendicular to the maximum horizontal principle stress in the area (Figure 4.10).

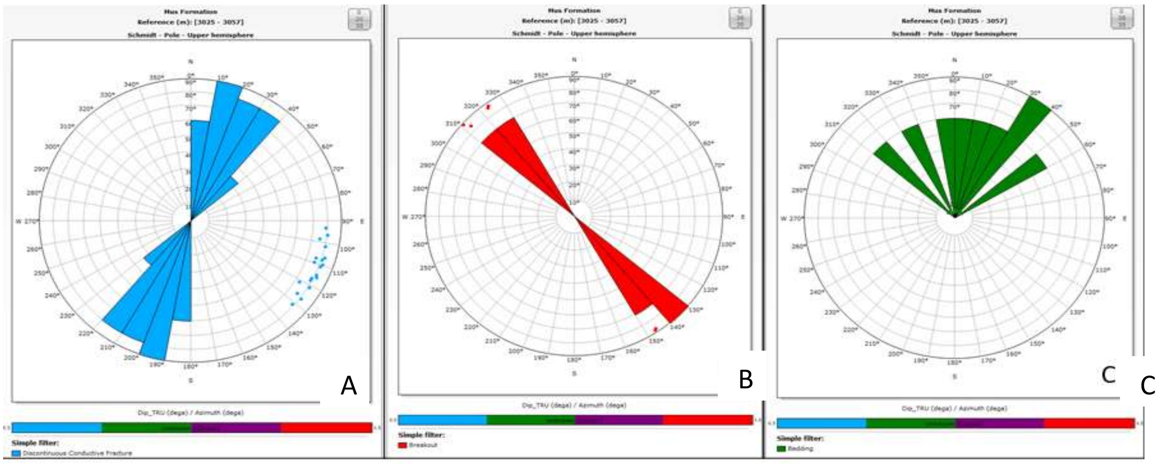

Figure 4.10: Rose diagrams showing the strikes of conductive fractures (A), borehole breakouts (B) and bedding planes dip direction (C), interpreted from FMI log in Well 4 within the Mus Formation

The FMI image quality is very good at the interval of the Mus Formation. This is primarily due to the FMI coverage of ~80% in the 8.5” hole size diameter. The caliper log shows in gauge hole at the most interpreted intervals (e.g. 2779m – 2798 m MD), except the lower part where Caliper 1 reads higher than Caliper 2 due to existence of borehole breakouts (Figure 4.11). Furthermore, fracture intensity is low (1 fractures/m) in some intervals, whereas same other intervals have even less fracture counts. The low fracture intensity could be attributed to the sub-sampling due to the vertical well trajectory and sub-vertical fracture orientation.

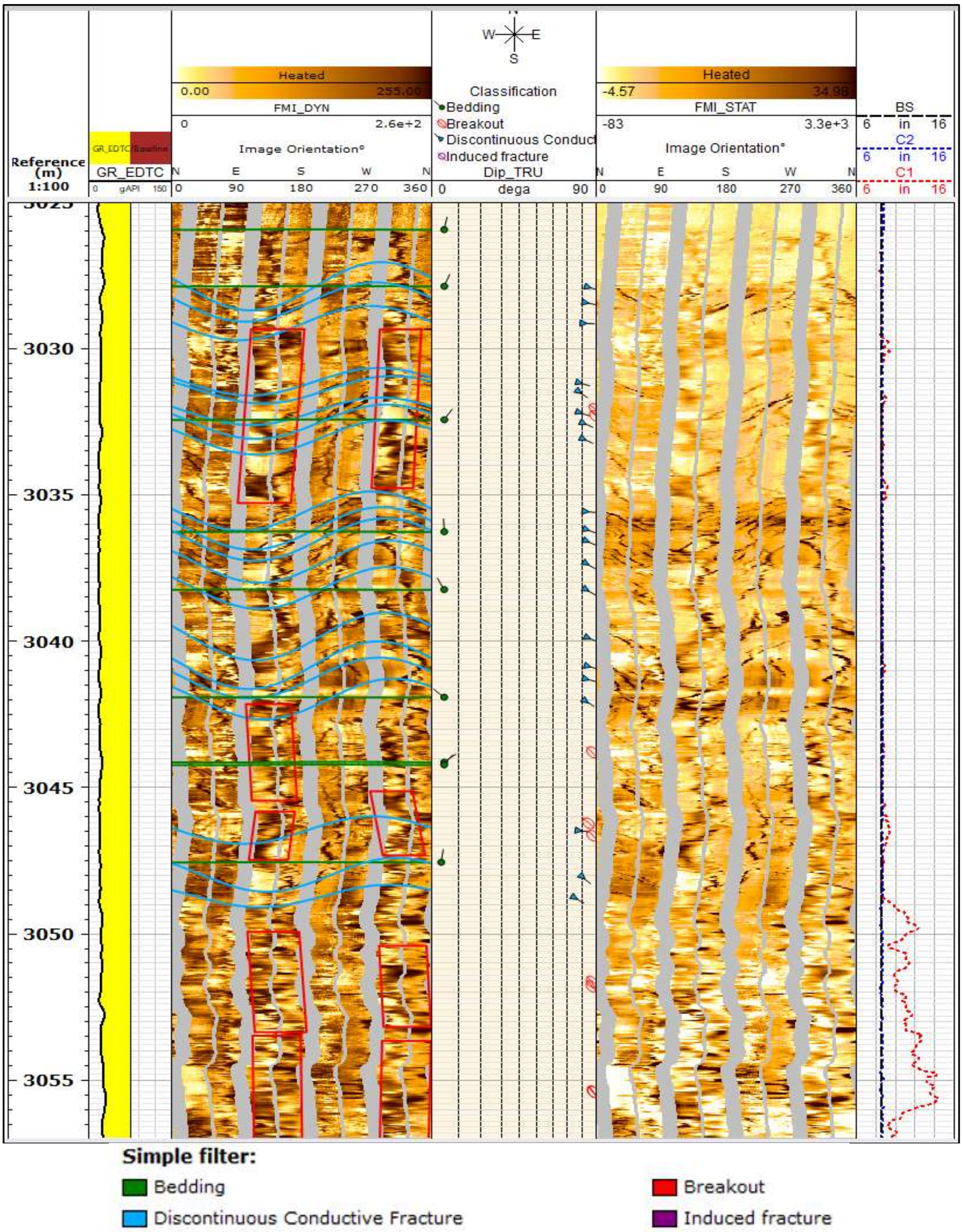

Figure 4.11: FMI static and dynamic logs showing beddings, conductive fractures and borehole breakouts interpreted from the FMI log in Well 4 within the Mus Formation. Note the caliper response against the borehole breakouts

4.6 Fracture Interpretation in Adaiyah Formation in Well 4

46 conductive fractures, drilling induced tensile fractures, borehole breakouts and bedding picks were interpreted within the Adaiyah Formation in Well4 bedding planes slightly tilted (<10º), due to crestal structural position of the well and dipping towards north (Figure 4.12). Conductive (open) fractures are highly dipping (65º-85º) comparing to bedding and their strike orientation is NE-SW. These open fractures are very important as they can provide essential permeability for fluid flow in Type II fractured reservoirs where matrix porosity is low. Furthermore, borehole breakouts have been also interpreted from the same interval. Borehole breakouts are wellbore instability fractures and they are oriented NW-SE which are perpendicular to the maximum horizontal principle stress in the area (Figure 4.12). Additionally, drilling induced tensile fractures which are also considered as wellbore instability fractures, have been interpreted and they are oriented NNE-SSW. Induced fractures are always oriented parallel to the maximum horizontal principle stress in the area (Figure 4.12).

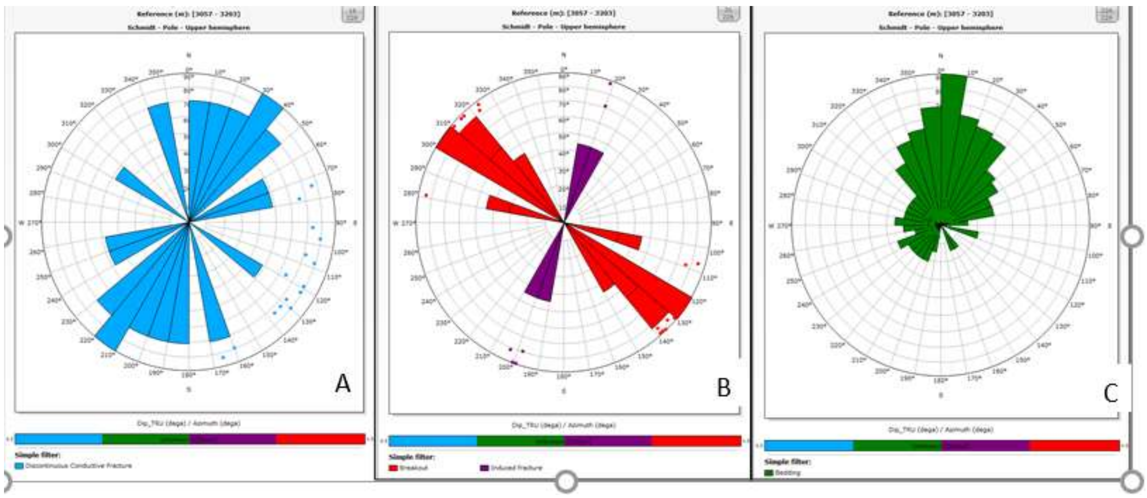

Figure 4.12: Rose diagrams showing the strikes of conductive fractures (A), borehole breakouts, drilling induced tensile fractures (B) and bedding planes dip direction (C), interpreted from FMI log in Well 4 within the Adaiyah

The FMI image quality is very good at the interval of the Adaiyah Formation. This is primarily due to the FMI coverage of ~80% in the 8.5” hole size diameter. The caliper log shows in gauge hole at the most interpreted intervals, except some parts where Caliper 1 reads higher than Caliper 2 due to existence of borehole breakouts (Figure 4.13). Furthermore, fracture intensity is very low. The low fracture intensity could be attributed to the sub-sampling due to the vertical well trajectory and sub-vertical fracture orientation. Figure 4.14 shows an example of the borehole breakout, whereas Figure 4.15 shows an example of a drilling induced tensile fracture.

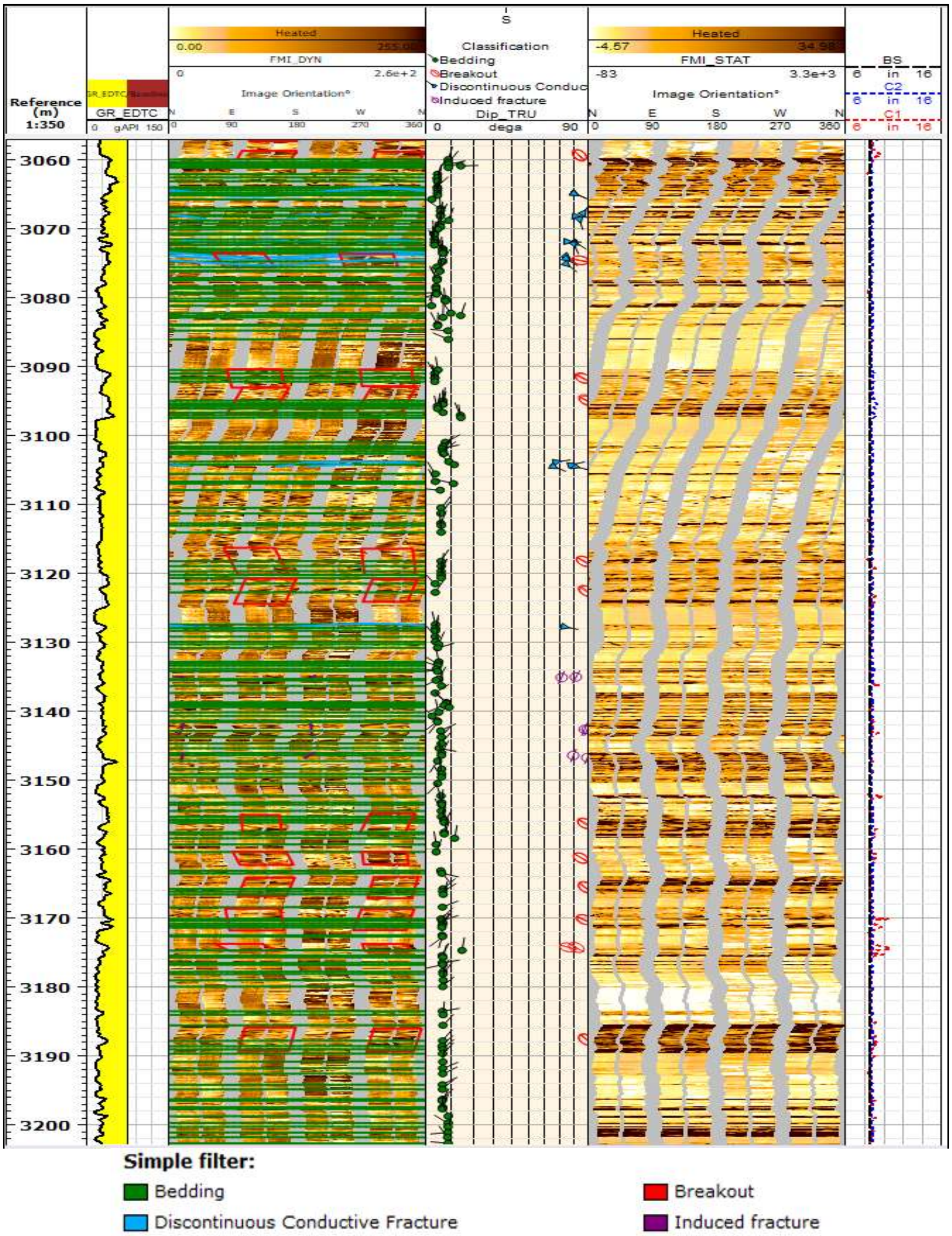

Figure 4.13: FMI static and dynamic logs showing beddings, conductive fractures &borehole breakouts interpreted from the FMI log in Well 4 within the Adaiyah Formation.

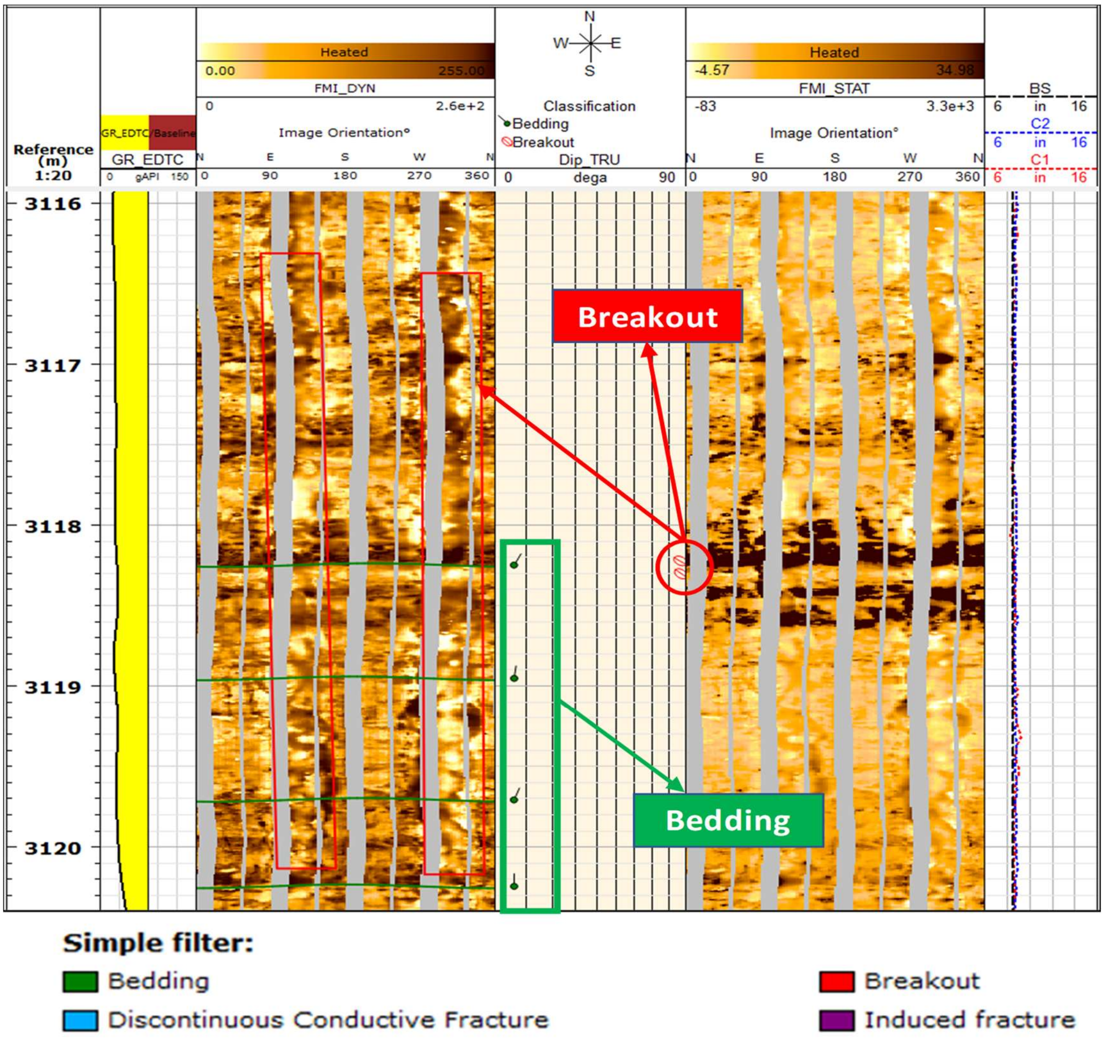

Figure 4.14: FMI static and dynamic logs showing beddings and borehole breakouts interpreted from the FMI log in Well 4 within the Adaiyah Formation

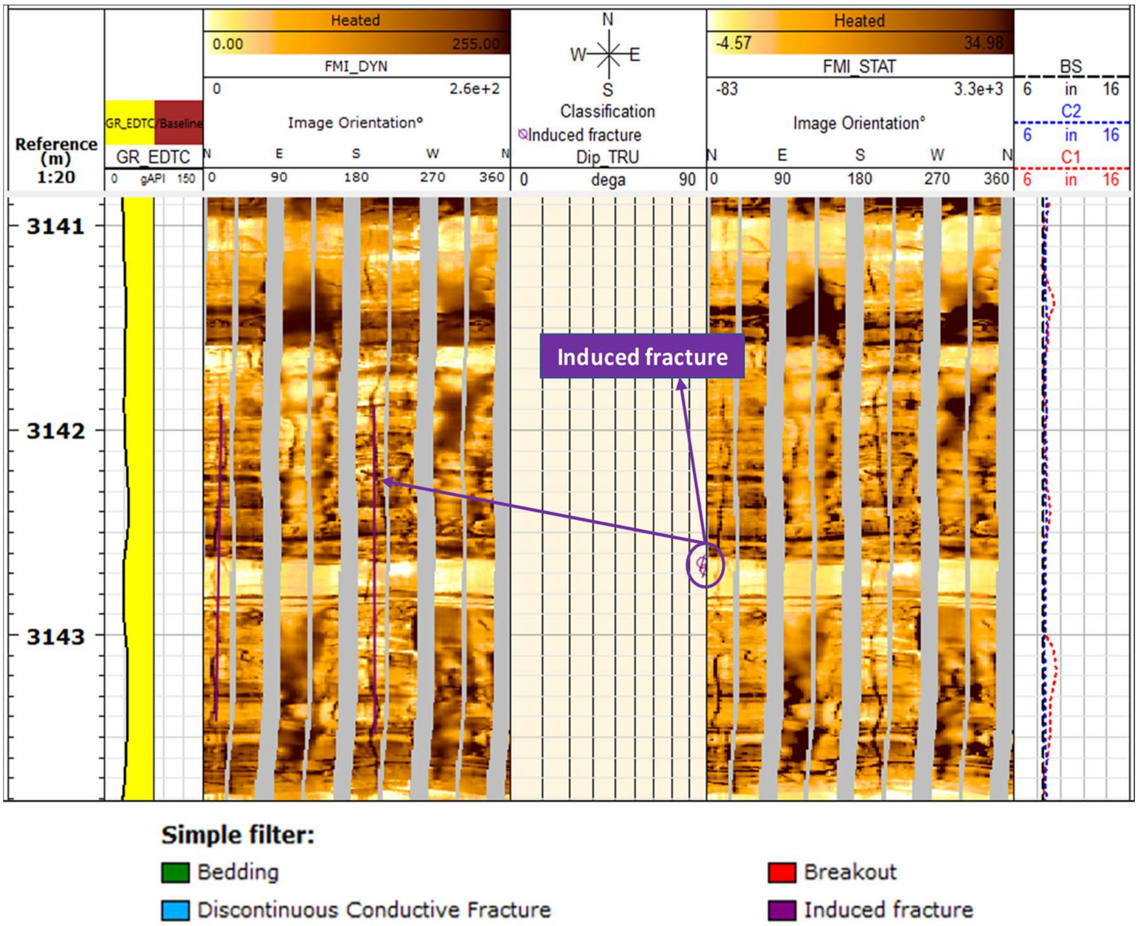

Figure 4.15: FMI static and dynamic logs showing drilling induced tensile fractures interpreted from the FMI log in Well 4 within the Adaiyah Formation

4.7 Integration of Well Data with Structure

The BHI interpretation was performed for three wells located on the crest of the anticlinal structure (Figure 4.16). Bedding planes in all three (Wells 2, 3 and 4)were observed to be gently tilted due to their crestal position with respect to the anticline. However, fracture intensity was different across the wells due to well trajectories (Wells2and 4) wells are vertical and Well3 is highly deviated with55º hole inclination and 283º hole azimuth. Fracture strike orientation in Well3 is oriented NNE-SSW and the hole azimuth is 283º (i.e. WNW-ESE). Thus, well trajectory has intersected maximum conductive fracture counts at high angle if not perpendicular. Furthermore, open fracture system seems to be better developed in the NW area of the structure. The NNE-SSW conductive fracture strike orientation in all interpreted three wells are perpendicular to the fold axis which is oriented WNW-ESE. This indicates that the permeability field might be anisotropic in this case, with the maximum fracture permeability in the NNE–SSW direction. Wells 2 and3, significant to moderate mud losses were reported in the upper parts of the Mus and Adaiyah formations (Figure 4.17). The mud losses are attributed to the open fracture system that have been interpreted from these wells.

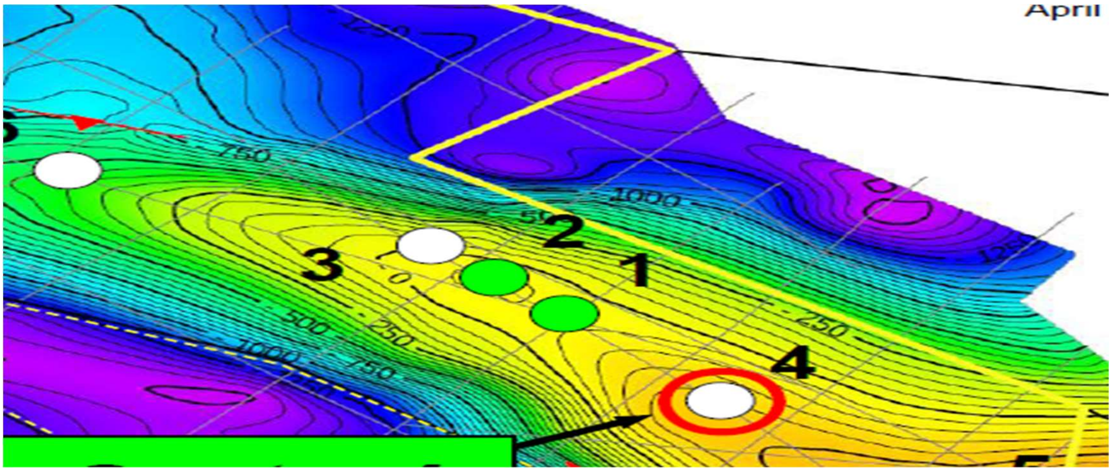

Figure 4.16: Mus-Adaiyah top structure map showing the well locations Well 2, Well 3 & the Well 4

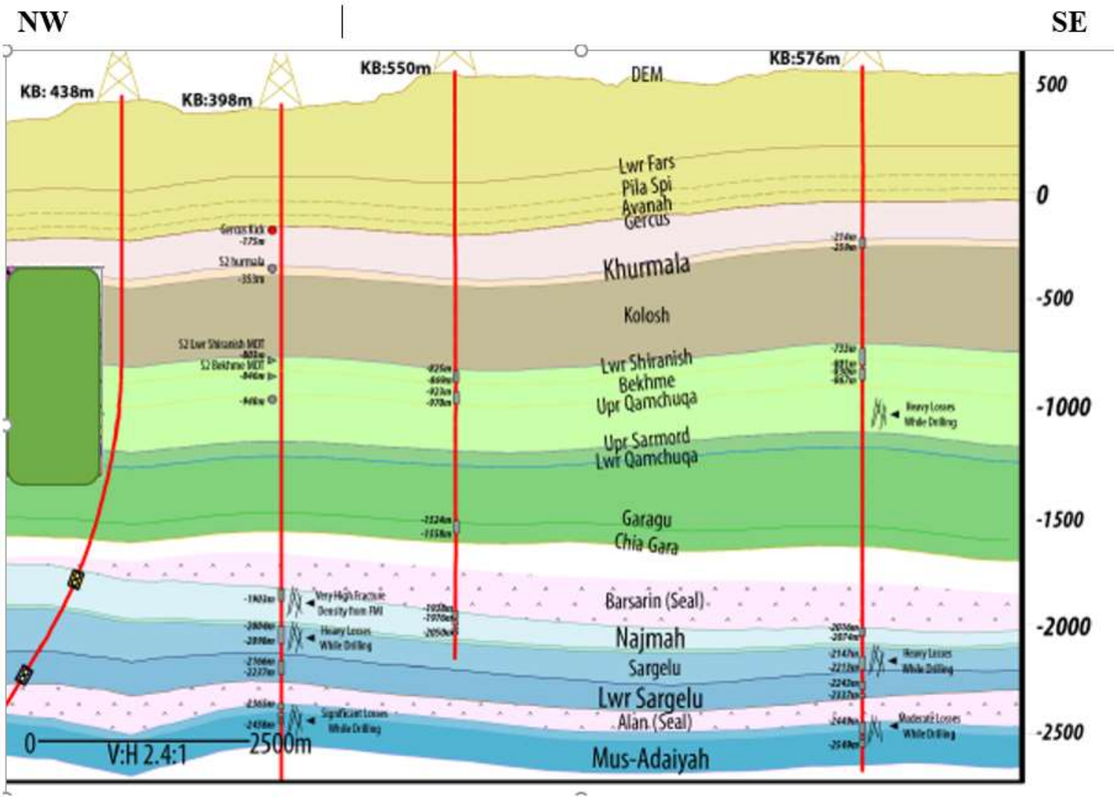

Figure 4.17: Geological cross-section showing the stratigraphic sequence in Wells 1, 2, 3 and 4.

CHAPTER 5
CONCLUSIONS AND RECOMMENDATIONS

5.1 Conclusions

- The conductive (open) fracture system in all three wells are striking NNE-SSW and this orientation is perpendicular to the fold axis, suggesting maximum fracture permeability in the NNE–SSW direction.
- Fracture intensity is much higher in the deviated well compared with vertical well. This is attributed to the sub-vertical fracture system and deviated well trajectory that intersected maximum fracture counts.
- Conductive (open) fracture system is better developed in the NW nose of the anticline compared to the SE region.
- Open fractures cannot be seen in seismic images as they are typically sub seismic in scale and have no displacement.
- Based on induced fractures measured in borehole image logs, the orientation of SHmax is estimated to be NE- SW direction.
- Due to the high horizontal stress in this field, a vertical well is more difficult to drill than inclined well.
- Excessive breakouts have obstructed successful evaluation of some sections of some wells.
- Minorborehole breakouts were interpreted in the Wells2 and 3 as they were drilled with efficient drilling fluids. However, several breakouts observed in Well 4 are due to drilling with higher mud weight.

5.2 Recommendations

- More deviated wells (50º-60ºhole inclination) with a hole azimuth-oriented WNW or ESE are required to drill in this field because it helps to encounter maximum fracture counts and to optimise production rate.
- Geomechanical model study is needed for wellbore stability assessment in the field.
- To avoid wellbore instability, its recommended to drilling in the WNW–ESE direction in order to keep the well trajectory normal to SHmax.
- It is recommended to drill slightly with lower mud weight for future drilling operation campaign to avoid borehole breakouts and drilling avoid induced tensile fracturing.
- Integration of fracture analysis from BHI should be integrated with seismic scale faults and fracture corridors for optimal well placement and drilling strategy.

REFERENCES

Akbar, M., and Sapru A.K. (1994). In-situ stresses in the subsurface of Arabian Peninsula and their effect on fracture morphology and permeability. *Abu Dhabi National Oil Company,* Society of Petroleum Engineers, 6th Abu Dhabi.

Akbar, M., and Sapru A.K. (1994). In-situ stresses in the subsurface of Arabian Peninsula and their effect on fracture morphology and permeability. *Society of Petroleum Engineering*, 17, 241-245.

Awdal, A. (2015). An Investigation of Fracture Patterns in Different Tectonic Settings. *Unpublished PhD Thesis, 29, 340-347.*

Antonellini, M.A., Aydin, A., and Pollard, D.D. (1994). Microstructure of deformation bands in porous sandstones at Arches National Park. *Journal of Structural Geology,* 16, 941-959.

Aydin, A. (1978). Small faults formed as deformation bands in sandstone. *Pure and Applied Geophysics,* 116, 913-930.

Bergbauer, S., and Pollard, D.D. (2004). A new conceptual fold-fracture model including pre folding joints based on the Emigrant Gap anticline. *Geological Society of America Bulletin,* 116, 294-307.

Bellen, Van., Dunnington, H.V., and Morton, D. (1959). *Lexique Stratigraphique Iraq* (pp. 333-351). Iraq.

Dershowitz, W., and Herda, H.H. (1992). Interpretation of Fracture Spacing and Intensity. *In Anonymous U.S. Symposium on Rock Mechanics* (pp 757-760). USA: University of Houston.

Donselaar, M. E., and J.M., Schmidt. (2010). The application of borehole image logs to fluvial facies interpretation. *American Association of Petroleum Geologists*, 92, 1-22.

Fossen H., and Hesthammer, J. (1997). Geometric analysis and scaling relations of deformation bands in porous sandstone. *Journal of Structural Geology,* 19, 1479-1493.

Fossen, H. (2010). Structural Geology. *Cambridge: Cambridge University.*

Fossen, H., Schultz, R.A., Shipton, Z.K., and Mair, K., (2007). Deformation bands in sandstone. *Journal of the Geological Society,* 164, 755-769.

Faraguna, J.K., Chance, D.M., and Schmidt, M.G. (1989). An improved borehole tele viewer system. *In SPWLA 30th Annual Logging Symposium*. Colorado: Society of Petrophysicists and Well-Log Analysts.

Gillespie, P.A., Johnston, J.D., Loriga, M.A., McCaffrey, K.J.W., Walsh, J.J., and Watterson, J. (1999). Influence of layering on vein systematics in line samples. *Journal of Geological Society,* 155, 35-56.

Gluyas, J. and Swarbrick, R. (2004). Petroleum Geoscience, *Blackwell Science* (pp.359-167).

Gas Barbier, M., Fauche, O., and Gaillard, C. (2010). Comparison between core and images in fracture networks knowledge. *International Proceeding Eurock, Cavtat* (pp. 29-31). Croatia.

Jassim, S. Z., and Buday, T. (2006). *Geology of Iraq. Prague*, Czech Republic.

Ladeira, F.L., and Price, N.J. (1981). Relationship between fracture spacing and bed thickness. *Journal of Structural Geology,* 3, 179-183.

Lambertini, R., Penolazzi, L., and Penolazzi, N. (1992). Fracture identification and quantification using borehole images. *In 2nd Latin American petroleum engineering conference proceedings* (pp. 89-95). Venezuela.

Narr, W., and Lerche, I. (1984). A method for estimating subsurface fracture density in core. Journal of American Association of Petroleum Geologists*,* 68, 637–648.

Narr, W., Schechter, D.W., and Thompson, L.B. (2006). Naturally Fractured Reservoir Characterization, *Journal of Society of Petroleum Engineers*, 27, 41-49.

Nelson, R.A. (2001). Geological analysis of naturally fractured reservoirs. *Journal of Gulf Professional Publishing, 16,320-*332

Nemati, M., and Pezeshk, H. (2005). Spatial distribution of fractures in the Asmari Formation of Iran in subsurface environment. *Journal of Natural Resources Research,* 14, 305-316.

Nicol A., Childs C., Walsh J.J., and Schafer K.W. (2013). A geometric model for the formation of deformation band clusters. *Journal of Structural Geology,* 55, 21-33.

Nixon C.W., Sanderson D.J., and Bull J.M. (2012). Analysis of a strike-slip fault network using high resolution multi beam bathymetry, *journal of offshore NW Devon U.K. Tectonophysics,*69, 541-543.

Newberry, B.M., Grace, L.M., and Stief, D.O. (1996). Analysis of Carbonate Dual Porosity Systems from Borehole Electrical Images. *In Permian Basin Oil and Gas Recovery Conference* (pp. 23-25). Texas.

Okubo C.H., and Schultz R.A. (2006). Near-tip stress rotation and the development of deformation band step over geometries in mode II. *Journal of Bulletin Geological Society of America* 118, 343-348.

Özkaya, S.I. (2002). Program to calculate magnitude and direction of maximum structural curvature and fracture-flow index. *Computer Geoscience* (pp. 399-407).

Pless, J.C. (2012). Characterizing fractured basement using the Lewisian Gneiss Complex, NW Scotland: Implications for fracture systems in the Clair Field basement. *Unpublished PhD Thesis, University of Durham*, 39,456-471.

Peacock, D.C.P. (2001). The temporal relationship between joints and faults. *Journal of Structural Geology,* 23, 329-341.

Peacock, D.C.P., and Mann, A. (2005). Evaluation of the controls on fracturing in the reservoir rocks. *Journal of Petroleum Geology,* 28, 385-396.

Pluijm, V.D., and Marshak, S. (2004). *Earth Structure.* New York NY, Norton & Company.

Price, N.J., and Cosgrove, J. (1990). *Analysis of geological structures*. Cambridge: *Cambridge* University.

Price, N.J. (1966). *Fault and joint development in brittle and semi brittle rocks*. Pergamon: Oxford.

Priest, S.D., and Hudson, J.A. (1976). Discontinuity spacing's in rock. *Journal of Rock Mechanics and Mining Science and Geomechanics Abstracts,* 13, 135-148.

Rashid, F., Hussein, D., Lawrence, J.A., and Khanaqa, P. (2020). Characterization and impact on reservoir quality of fractures in the cretaceous, Zagros folded belt. *Journal of Marine and Petroleum Geology*, 10,14-17.

Ramsey, J.M., and Chester, F.M. (2004). Hybrid fracture and the transition from extension fracture to shear fracture, *Journal of Geologic Nature,* 428, 63-66.

Reinecker, J., Mark, T., and Birgit, M. (2003). Borehole breakout analysis from four arm caliper logs. *Journal of Geological Science London*, 48, 305-325.

Ramsay, J.G., and Huber, M.I. (1987). *The techniques of modern structural geology*. London: Academic Press.

Sanderson, D.J., Nixon, C.W. (2015). The use of topology in fracture network characterization. *Journal of Structural Geology*, 12,123-129.

Sullivan, K.B., and Schepel, K.J. (1995). Borehole image logs applications in fractured and thinly bedded reservoirs. *In Society of Petro physicists and Well Log Analysts 36th Annual Logging Symposium.* Paris: Society of Petro physicists and Well-Log Analysts.

Twiss, R.J., and Moores, E.M. (1992). *Structural Geology*. New York: W.H. Freeman.

Twiss, R.J., and Moores, E.M. (2007). *Structural Geology*. New York: W.H. Freeman.

Underwood, C.A., Cooke, M.L., Simo, J.A., and Muldoon, M.A. (2003). Stratigraphic controls on vertical fracture pattern I Silurian dolomite. *Journal of American Association of Petroleum Geologists*, 87, 121– 141.

Wanless, H.R. (1979). Limestone response to stress pressure solution and dolomitization. *Journal of Sedimentary Research,* 49, 122-131.

Wong, S.A., Startzman, R.A., and Kuo, A. (1989). New approach to the interpretation of wellbore images. *In SPE annual Technical conference and Exhibition proceeding* (pp. 73-82). Taxes.

Wennberg, O.P., Azizzadeh, M., Aqrawi, A.A.M., Blanc, E., Brockbank, P., Lyslo, K.B., Pickard, N., Salem, L.D., and Svana, T. (2007). The Khaviz Anticline an outcrop analogue to giant fractured Asmari Formation reservoirs in SW Iran. *Journal of Geological Society Special,* 270, 23-42.

Williams, P.D., Maddock, R.H., Sapru, A.K. and Lawrence, M.J.F. (2000). Analysis of a Fractured Carbonate Reservoir Using Borehole Images. *In Abu Dhabi International Petroleum Exhibition and Conference*. Abu Dhabi: Society of Petroleum Engineers.

Wu, H., and Pollard, D.D. (1995). An experimental study of the relationship between joint spacing and layer thickness. *Journal of Structural Geology,* 17, 887-905.

Yildirim, A., and Goodliffe, A. M. (2014). Subsurface Fracture Analysis Using FMI Logs Implications for Regional State of Stress Prediction in the Black Warrior Basin, Alabama, USA. *In International Conference and Exhibition*. Istanbul: E&P Geoscientist.

APPENDICES

APPENDIX 1

TURNITIN SIMILARITY REPORT

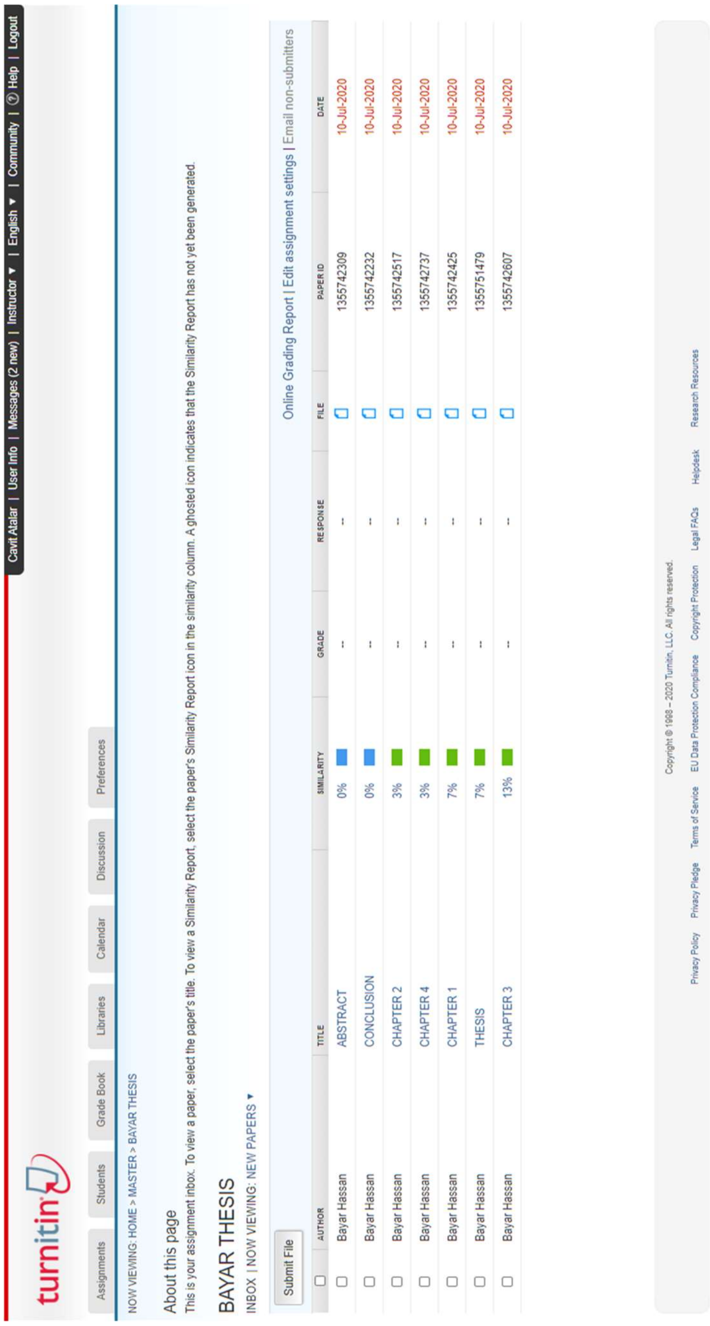
Cavit Atalar | User Info | Messages (2 new) | Instructor ▾ | English ▾ | Community | Help | Logout

Assignments | Students | Grade Book | Libraries | Calendar | Discussion | Preferences

NOW VIEWING: HOME > MASTER > BAYAR THESIS

About this page

This is your assignment inbox. To view a paper, select the paper's title. To view a Similarity Report, select the paper's Similarity Report icon in the similarity column. A ghosted icon indicates that the Similarity Report has not yet been generated.

BAYAR THESIS

INBOX | NOW VIEWING: NEW PAPERS ▾

Submit File

Online Grading Report | Edit assignment settings | Email non-submitters

AUTHOR	TITLE	SIMILARITY	GRADE	RESPONSE	FILE	PAPER ID	DATE
Bayar Hassan	ABSTRACT	0%	--	--		1355742309	10-Jul-2020
Bayar Hassan	CONCLUSION	0%	--	--		1355742232	10-Jul-2020
Bayar Hassan	CHAPTER 2	3%	--	--		1355742517	10-Jul-2020
Bayar Hassan	CHAPTER 4	3%	--	--		1355742737	10-Jul-2020
Bayar Hassan	CHAPTER 1	7%	--	--		1355742425	10-Jul-2020
Bayar Hassan	THESIS	7%	--	--		1355751479	10-Jul-2020
Bayar Hassan	CHAPTER 3	13%	--	--		1355742607	10-Jul-2020

Prof, Dr, Salih SANER
Thesis Supervisor
12.08.2020

APPENDIX 2

ETHICAL APPROVAL DOCUMENT

YAKIN DOĞU ÜNİVERSİTESİ

ETHICAL APROVAL DOCUMENT

Date: 07/08 /2020

To the **Graduate School of Applied Sciences**

The research project titled " **… Fracture Analysis of Mus and Adaiyah Formations Using Borehole Image Logs, Zagros Belt, North of Iraq .**'' has been evaluated. Since the researcher will not collect primary data from humans, animals, plants or earth, this project does not need through the ethics committee.

Title:

Name Surname: Prof. Dr. Salih SANER

Signature:

Role in the Research Project: Supervisor

Title:

Name Surname:

Signature:

Role in the Research Project: